Nuclear radiation detectors based on plastic scintillators

Yu. K. Akimov
Joint Institute for Nuclear Research, Dubna

Fiz. Elem. Chastits At. Yadra **25**, 496–549 (March–April 1994)

The current situation regarding the measurement of the energy and ionization losses of nuclear radiation using detectors with plastic scintillators is reviewed. The dependence of the pulse height of a plastic scintillation counter on various factors is described. Special attention is paid to the technique of scintillation light collection using light guides containing wavelength shifters. A large part of the review is devoted to the use of plastic scintillators in the construction of hadron and electromagnetic calorimeters.

1. INTRODUCTION

The early period of the development of detectors based on the use of both inorganic and organic scintillators has been described most completely in the fundamental study by Birks.[1] A special monograph has been devoted to the use of organic scintillators in high-energy physics experiments.[2] Later developments in organic scintillator technology occurring in the 1960s and 1970s are described in the reviews of Refs. 3 and 4. During this period there was great progress in the use of such valuable features of organic scintillators as their fast speed of response and the possibility of using them to build rather large and relatively inexpensive detectors. The most noteworthy recent development has been the ever-increasing use of plastic organic scintillators for measuring the energy of particles, particularly in wide-aperature and large-scale setups. This is the subject of the present review. The technology of coordinate and time measurements lies outside its scope.

In Sec. 2 we consider the phenomena determining the pulse height at the output of the relatively thin scintillation counters commonly used to determine the location and time of the passage of charged particles, and also for their identification in some cases. Here we describe the fluctuations of the ionization losses, the techniques of light collection by means of spectrum shifters and from thin counters, and also the effect on the scintillator light yield of various external factors like the temperature, aging, the presence of a magnetic field, and, in particular, radiation. Section 3 is devoted to the spectrometry of charged particles of intermediate and low energy. Here we describe total-absorption detectors made only from scintillating material, phoswich detectors, the detection of low-energy ions and electrons, and pion detectors. In Sec. 4 we discuss the spectrometry of high-energy particles, where a scintillator is alternated with a denser, passive material for particle absorption. The scintillator in such a detector (calorimeter) can be of the form of plates or fibers.

2. PLASTIC SCINTILLATION COUNTERS

Some general remarks

Organic scintillators take the form of crystals (anthracene, stilbene), or liquids, or plastics. Among the basic characteristics of scintillators are the conversion (scintillation) efficiency η or the light yield measured at the photosensitive surface, and the luminescence (emission) time τ. The scintillation efficiency gives the fraction of ionization losses of the particle that has gone into the formation of the scintillation burst. For anthracene, $\eta_a=0.04$ (Ref. 1). The typical values of η for other organic scintillators are 45–70% of η_a (Ref. 4).

Plastic scintillators have become the most widely used in physics experiments. They are made from hydrocarbon solvents with the appropriate scintillating impurities, which are referred to by various names in the literature: fluorescing dyes, luminophores, fluors, fluorescents, and "dopants."

Scintillators based on the use of polystyrene (PS) or polyvinyltoluene (PVT) as solvents have small luminescence times ($\tau \lesssim 3$ nsec). Acrylic solvents (polymethylmethacrylate—PMMA and so on) can be used to make inexpensive scintillators, although in speed of response ($\tau \sim 10$ nsec) and light yield they are inferior to the types of scintillators mentioned above.

The scintillation efficiency depends on the ionization density. The tabulated data on η refer to minimally ionizing particles. As the specific ionization dE/dX grows, the light yield falls according to the law $\eta' = \eta(1+\mathrm{KB}\, dE/dX)^{-1}$, where KB is the Birks parameter depending on the type of scintillator (see Sec. 4).

Energy losses of a charged particle in a layer of detector material

The energy losses of a charged particle in the passage through the detector material arise from ionization processes, radiation and Čerenkov emission, and nuclear interactions. Ionization losses dominate for particles of mass m many times greater than the electron mass m_e. The value of the specific ionization losses dE/dX is proportional to the square of the particle charge z and is a function of the particle speed β. As β increases, dE/dX first decreases, reaching a minimum near $\beta=0.95$ (as a fraction of the speed of light c), and then again increases, but considerably more slowly.

Ionization losses of a particle in a layer of absorber material X arise as a result of collisions of the particle with interatomic electrons. The statistical nature of these interactions leads to fluctuations of the energy loss, which were first calculated for "thin" absorbers by Landau.[5] An absorber is described as "thin" if the energy of a particle

 1063-7796/94/020210-24$10.00

TABLE I. Most probable energy losses Δ_p and total widths at half-max FWHM for $X=1040$ μm of silicon for various $\beta\gamma$.

$\beta\gamma$	2,1	8,5	14	57	3914	15700
Δ_p, keV	323	307	308	315	320	320
FWHM, keV	93,1	86,5	84,2	85,4	86,5	85,7
FWHM/Δ_p, %	28,8	28,2	27,3	27,1	27,0	26,8

which has passed through it can be considered unchanged. The problem of the fluctuations of the ionization losses was then solved more accurately by Vavilov.[6] Whereas in the Landau solution a freed electron can have any energy from zero to infinity, Vavilov restricted the maximum energy transferred to the electron to the kinematical limit: $\varepsilon_{\max}\approx 2m_e c^2\beta^2/(1-\beta^2)$. The degree of fluctuations of the ionization losses can be defined as the characteristic quantity $\kappa\equiv\xi/\varepsilon_{\max}$, where $\xi=0.30058\ m_e c^2(Z/A)Xz^2$. Here Z is the atomic number and A is the atomic mass of the material and z is the particle charge. The Vavilov solution was then improved by Shulek *et al.*[7] by including long-range collisions of the charged particle with electrons bound in atoms of the stopping matter. Strictly speaking, the Landau solution pertains to the case where $\kappa=0$, which follows from the condition $\beta_{\max}=\infty$. However, already for $\kappa<0.1$ the Landau distribution differs little from the Vavilov distribution, since the most probable energy lost by the particle Δ_p turns out to be much smaller than the maximum possible energy $\xi_{\max}$ transferred to a δ electron.

For $\kappa<1$ a prominent feature of the ionization-loss spectrum is the contribution of electrons with relatively high energy (δ electrons), which appears as a tail at large losses. The experimental data have been obtained mainly for silicon detectors, which allow more accurate energy measurements to be carried out. However, there is no clear reason why it would not be possible to apply the results of these measurements to scintillation counters, at least for making rough estimates. It should also be born in mind that in a scintillator the ionization for thickness X corresponding to the same weight is roughly 25% higher than in silicon, which follows from the atomic structure of these materials.

In Table I we give[8,9] the experimental data on the loss spectra of particles with various $\beta\gamma$ in silicon of thickness 1040 μm, which in energy loss is equivalent to a plastic scintillator with $X_c=1934$ μm; here $\gamma=(\sqrt{1-\beta^2})^{-1}$.

A slight decrease of the relative value of the halfwidth at half-max of the spectrum with increasing $\beta\gamma$ is seen. However, this does not indicate an actual narrowing, but is the result of the lengthening of the spectrum tail. For large $\beta\gamma$ beginning at about 100, Δ_p and the FWHM remain practically constant.

Measurements show that the observed ionization-loss spectra for thin ($X<200$ mg/cm^2) absorbers are considerably broader than the Landau or Vavilov distributions. An analytic description of the spectra is best obtained by the convolution method suggested by Bichsel.[9] The energy loss process undergone by a charged particle in a thin layer of absorber is described most accurately by the Monte Carlo method,[10] which is applicable for Si (Ref. 11) at $X=1$–100 μm.

Good agreement has been obtained with the experimental data available for $X>30$ μm and large $\beta\gamma$ (Ref. 8). For $\beta\gamma>100$ the values of Δ_p and FWHM for $X=3$–2905 μm are given in Table II. The data for $X=3$–20 μm were calculated,[11] and the others are from experiment;[8] the data for $X=2905$ μm were obtained in Ref. 12.

The departure of δ electrons from the detector leads to a contraction of the spectrum of ionization losses deposited in it and slightly changes it toward a Gaussian distribution. However, this has little effect on the values of Δ_p and the FWHM (Ref. 11). As an example, in Fig. 1 we show the spectrum measured for cosmic muons by a 1-cm-thick scintillation counter.[13] The solid line was calculated excluding all events in which $\xi>1.5$ MeV. We see that the agreement between the calculated and experimental data is good.

Naturally, the presence of a tail in the ionization-loss spectrum interferes with the separation of particles using the measured losses. The separation can be improved considerably by measuring the ionization simultaneously in several counters.[14] However, the process of pulse formation in adjacent counters is to some degree correlated be-

TABLE II. Dependence of Δ_p and FWHM on the absorber thickness X for $\beta\gamma>100$.

X, Si, μm	3	5	10	20	32	51	100	174	290	1040	2905
Δ_p, keV	0,42	0,82	1,87	4,2	7,1	12,3	26,8	48,2	81,0	320	943
Δ_p/X, keV/mm	140	164	187	210	222	242	268	277	279	308	325
FWHM, keV	0,75	1,1	1,8	3,4	5,5	7,7	14,0	21,6	30,2	86,5	245
FWHM/Δ_p, %	179	134	96	81	77	63	52	45	37	37	26
X scint., μm	5,6	9,3	18,6	37,2	59,5	94,8	186	324	540	1934	5403

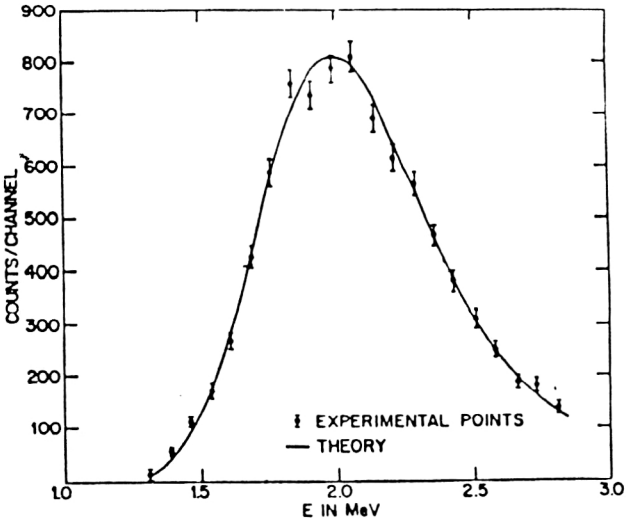

FIG. 1. Energy losses deposited by cosmic-ray muons in a plastic scintillator of thickness 1 cm (Ref. 13).

cause of the δ electrons created in one counter and travelling to another. This worsens the conditions for particle separation.

Light collection

The most common shape of relatively thin ("straight-through") scintillators is that of a parallelpiped with polished sides on which total internal reflection of light occurs. For ideally smooth walls and no absorption in the scintillator volume, the fraction of light collected on one wall is 0.5 $(5\cos\varphi_0-3)$, where φ_0 is the angle of total internal reflection at the scintillator-air boundary.[15] For two facing walls this fraction is $2\cos\varphi_0-1$. In actual extended scintillators with limited transparency light loss occurs, and the light lost is primarily the part which travels the longest distance to the light-collecting surface. Here the amount of collected light is mainly determined by the part which falls in a cone of angle $\theta_{\max}=2(\pi/2-\varphi_0)$ opening toward the light-collecting surface. Irregularities (roughness) of the reflecting surfaces leads to the knockout of light rays from this cone and their subsequent loss. However, regarding irregularities, it should be noted that a really negative effect is produced only by those which point along the axis of the light-collecting cone. A deviation from planarity in the transverse direction is allowed. This can be seen, in particular, in the example of scintillation plates prepared by the extrusion method: extraction from a softened mass. Here the plates are slightly ribbed, but in the longitudinal direction their uniformity is very high, which ensures a sufficiently large attenuation length Λ_0 (the amount of light decreases by a factor of e over a distance Λ_0). For example, in a blue scintillator (with POPOP as the fluorescing impurity) of thicknesses 10 mm and 5 mm a value $\Lambda_0=1.8$ m was obtained.[16] The fact that the same result was obtained for the smaller thickness as for the larger one indicates the high quality of the scintillator surface. In fact, the losses due to imperfection of the surface would depend on the number of light reflections from this surface, which is inversely proportional to the thickness of the scintillation plate. In a green scintillator (with pyrazoline as the impurity), Λ_0 increased to 2.4 m.

When using scintillators of large dimension with polished surfaces, it is necessary to increase the scintillator thickness in order to decrease the number of reflections. For example, for a length of 3 m the thickness should be 3 cm. Naturally, for such lengths it is necessary to choose scintillators with small absorption inside the volume. A scintillator of the type NE 114 manufactured by the Nuclear Enterprises Company of Great Britain has a large volume absorption length $\Lambda_0=4$ m. Its light yield is half of that of anthracene. The same Λ_0 but a light yield 25% higher has been reported in Ref. 17 for a scintillator of the type UPS 9323A (Khar'kov, Ukraine). The authors attribute these characteristics to the high quality of the basic material, polystyrene.

Almost half the light from points lying near the light-collecting surface can fall on this surface directly, without reflection from the lateral walls. The resulting nonuniformity can be decreased if the scintillator is connected to a photocathode via a light guide of length $l>d\tan\varphi_0$, where d is the diagonal of the output face of the scintillator.[15] Here it is assumed that the light guide serves as a direct extension of the scintillator. The index of refraction of the light guide n_g is different from that of the scintillator n_s. The usual material of which light guides are made—organic glass (plexiglass, lucite)—has $n_g=1.49$, while a polystyrene scintillator has $n_s=1.59$. When a light guide is connected to a scintillator the solid angle of the light-emission cone decreases by $\sim 30\%$. Acrylic scintillators have the same index of refraction as light guides, i.e., they are completely optically compatible with them if, of course, the scintillator and the light guide are connected using optical lubricant or glue with the same n.

The light guide must transport the light from the scintillation surface, which usually has the form of a long, narrow rectangle, to the spherical photocathode of the photomultiplier. A smooth transition from a rectangular cross section to a spherical one is obtained, for example, by making the light guide in the form of a fish tail. For light transport with minimum loss by such a light guide it is necessary for the cross section to be constant along its axis (it cannot decrease).[18]

Light guides made of strips of organic glass connected in the form of a fan have become widespread.[19] They are made by twisting and bending the strips, which are softened by heating to 140–150 °C. The advantage of such light guides over those in the shape of a fish tail is clearly manifested when the light-collecting faces of the scintillator are large. They are distinguished by high uniformity of the light collection and ensure that the times for the light to arrive at the photocathode from all segments of the light-collecting surfaces of the scintillator are the same.

Fiber-optics light guides are used in those cases where photomultipliers must be placed rather far from the scintillators. A fiber consists of a core and a cladding, with the index of refraction of the core n_1 larger than that of the

cladding n_2. If the light travels at an angle $\theta < \theta_{max} = \pi/2 - \arcsin n_2/n_1$, it undergoes total internal reflection at the core-cladding interface and propagates along the fiber. Light rays with $\theta > \theta_{max}$ enter the cladding and are reflected at the cladding-air interface if $\theta < \pi/2 - \arcsin n_1$, i.e., they also will propagate along the fiber. However, the outer surface of the cladding is less perfect and for large θ the number of reflections is large, so the "cladding" light is attenuated rather rapidly. It can be eliminated entirely by blackening the outer surface of the fiber.

Fibers can be used to make long, flexible light guides. For example, in Ref. 20 a light guide of diameter 2 mm had a length of 3 m and a light capture angle of $\theta_{max} = 31°$. The core was made of PMMA ($n_1 = 1.495$) and a polymer cladding with $n_2 = 1.4027$ was used. Light was transported from a BC-412 scintillator, whose emission spectrum has a maximum at $\lambda = 434$ nm. The light attenuation in the light guide was less than 3%/m. The scintillator dimensions were $180 \times 5 \times 1$ cm. The signal amplitudes for scintillator points 20 and 180 cm away from the light guide were compared. At the farthest point minimum ionizing particles produced 20 photoelectrons. The signal from the closest point was 1.8 times higher. Without the light guide the signal amplitudes differed by a factor of 2. The attachment of the light guide decreased the distance between the points owing to the elimination of rays with large θ. Naturally, here the signal amplitude was decreased.

Light collection from very thin scintillation plates

The number of light reflections from the scintillator walls grows with decreasing scintillator thickness. Nonuniformities in the thickness lead to a significant increase of the light escaping through the lateral walls. This is especially clearly manifested for small thicknesses ($X < 1$ mm). To direct this sideways-emitted light toward the photomultiplier, the scintillator is connected to a cavity with reflecting walls. In the simplest case this can be simply a "roof" of aluminum foil as, for example, in Ref. 21. However, higher light collection albeit with smaller time spread is obtained using hemispherical[22,23] or toroidal[24] structures.

The need for very thin counters ($X < 100\ \mu$m) arises in those cases where the energy losses and multiple Coulomb scattering arising in the passage of charged particles through these counters must be minimal. Naturally, the amount of passive material in the particle path also must be reduced to a minimum. This is especially important at low energies and/or high z of the detected particles. As an example, in Fig. 2 we show the construction of a counter[22,23] used in measurements in a beam of antiprotons with $E < 175$ MeV (Ref. 25). The plastic scintillator (NE 102) is made in the form of a disk of diameter 2 cm. Counters of various thicknesses were studied, the minimum being 10 μm. This scintillator was placed in a hemispherical aluminum cavity on a polished aluminum holder. Two aperatures for the beam to pass through were made in the hemisphere. After reflection on the aluminum the light reaches the light guide ($n = 1.5$), and then the photocathode of an XP2020 photomultiplier. The optimal dimensions of the construction elements were found by Monte Carlo modeling. Experience showed that a reflector covered with vaporized aluminum is more efficient than aluminum which was simply polished. Whereas the latter has a reflection coefficient of 70% at a wavelength of 406 nm, the vaporized aluminum allows the reflection coefficient to be increased to 92%. The spectrum of pulses from the scintillation counter measured in a 38.5-MeV proton beam had an average value of $\Delta E = 14$ keV and a clearly expressed maximum at $X = 10\ \mu$m. During operation of the photomultiplier in the single-electron mode the pulse-coincidence efficiency of this counter and a different one with a thicker scintillator was close to 100%.

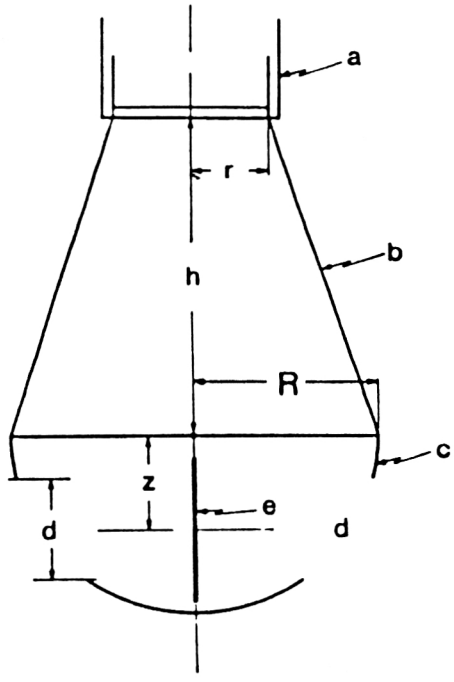

FIG. 2. Detector geometry: (a) Photomultiplier, (b) light guide, (c) hemispherical reflector, (d) aperature of diameter 2.8 cm, (e) thin scintillator; $R = 5$ cm, $z = 2.6$ cm, $h = 9$ cm, $r = 2.2$ cm (Ref. 23).

Light guides with emission-spectrum shifters

In many modern experiments it is necessary to collect light from scintillators of a large area. The use of a large number of photomultipliers is expensive and often simply too difficult. At the expense of considerable loss of light the detector construction can be made considerably less expensive and simplified if light guides with wavelength shifters (WLSs) are used.[26–31] Two types of spectrum-shifting light guides arose simultaneously in physics experiments: one in the form of a block located on the light-collecting face of a scintillation plate,[29] and the other in the form of a rod passing through holes made in the scintillation plates (see Fig. 3).[30] The operating principle of the two constructions is the same. In both the light guide is separated from the scintillator by a small air gap. The transverse cross section of the light guide corresponds to the area of the photodevice (a photomultiplier or photocathode) connected to it. The walls of the light guide are polished. Light arriving at

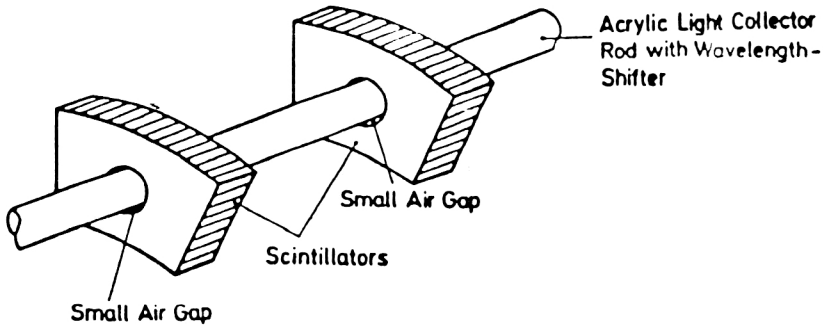

FIG. 3. Structure with a spectrum-shifting light guide in the form of a rod passing through a hole in the scintillators (Ref. 30).

the light guide from the scintillator is absorbed by the shifter and reemitted as light of longer wavelength. This reemission is isotropic, and owing to total internal reflection on the walls of the light guide the corresponding part of the light is directed toward the photodevice. The presence of the air gap between the light guide and the scintillator is crucial for the light transport along the light guide. Otherwise, the reemitted light would travel back into the scintillator. Of course, there is much less light at the face of the light guide than comes from the scintillator. The air gap creates two interfaces at which a significant fraction of the original scintillator light is lost, and the part of the reemitted light which is not captured by total internal reflection is lost. There are two more factors which lead to a decrease of the amplitude of the signal from the photomultiplier. One is that its spectral sensitivity to the longer-wavelength (usually green) reemitted light is lower than that to the original (blue) light. In addition, the latter is not completely captured, since the concentration of WLS inside the light guide is limited so that the attenuation of remitted light on the path to the photomultiplier is small.

Among the first and then widely used WLSs is BBQ (Benzimidazobenzisochonolin-7-on), the emission spectrum of which has a maximum near 495 nm. In one of the early calorimeters (see Sec. 4) a light guide of acrylic plastic of dimensions $2\times4\times150$ cm contained BBQ with a concentration of 90 mg/l (Ref. 29). For this BBQ concentration the attenuation length Λ_0 of the reemitted light was 3 m. Placement of a mirror at the end of the light guide opposite to the photomultiplier raised the effective length Λ_0 to 5 m. The uniformity of the light guide was improved by the introduction in front of the photomultiplier of a filter eliminating the short-wavelength component of the light below 430 nm. This wavelength range overlaps with the BBQ absorption spectrum and its fraction grows in approaching the photocathode, which without the filter would increase the nonuniformity. The light guide was wrapped on three sides with aluminum foil for reflecting the light escaping from it. The BBQ shifter absorbed about 70% of the blue light incident from the scintillator. The authors estimated that the light-collection efficiency by light guides with WLSs is 12% of the efficiency of an ideal system in which blue light would be transported by "pure" adiabatic light guides optically connected to the scintillator and photomultipliers. The placement of acrylic blocks with WLSs on all four sides of the scintillator raised both the efficiency and the uniformity of the light collection.

The number of photomultipliers in a detector made from stacks of scintillator plates can be decreased further by reemitting the light in two stages.[32] The first spectrum-shifting light guide is placed along the edge of the scintillator, and the second is placed perpendicular to the first, at the corners of the scintillators. A system has been studied in which the plate thickness was 1 cm and the cross section of the second light guide is 1 cm^2; it was connected to an XP2013 photomultiplier sensitive to red light. The measurements were carried out using various WLS combinations. The maximum signal was obtained for the combination BBQ+Yellow 323. The absorption and emission peaks of Yellow 323 respectively lie at 525 and 600 nm. The passage of minimally ionizing particles through the scintillator is accompanied by the production of 5 photoelectrons on the average. A somewhat smaller number of photoelectrons (3.7) was observed for a different combination: coumarin (7-dietylamino-4-methanmarin) and K-27 (xantheneacid derivative). The absorption peak in coumarin is located at 360 nm, and the emission peak is at 410 nm. The K-27 shifter efficiently absorbs light in this region and emits light near 495 nm (see Fig. 4); the center of gravity of the emission spectrum is at 525 nm. The advantage of this combination over BBQ+Yellow 323 is the large optical attenuation length. Whereas $\Lambda_0=45$ cm is obtained using Yellow 323, $\Lambda_0=100$ cm is obtained with K-27.

Double shifters have also been made using fiber optics.[33,34] Fiber light guides with WLSs can be used to construct the most compact light-collection systems. For this the fiber is forced directly into the volume of the scintillator, but without optical contact, so that the fiber and the scintillator are separated by air. In Fig. 5 we show some versions of this construction. In the first two[35] the grooves for the fibers are made on the face of the scintillation plates, while in the third they are on the end of a scintillator of thickness 3 mm (Ref. 36). The fiber diameter was 1.5 mm. The material of the fiber core was polystyrene ($n_1=1.59$) with the addition of K-27 (20 mg/l in Ref. 36), and the cladding was made of polyvinyl acetate ($n_2=1.46$). The light falling in a cone of opening angle 23° was collected. The light attenuation length was greater than 10 m. The typical quantum efficiency of the photo-

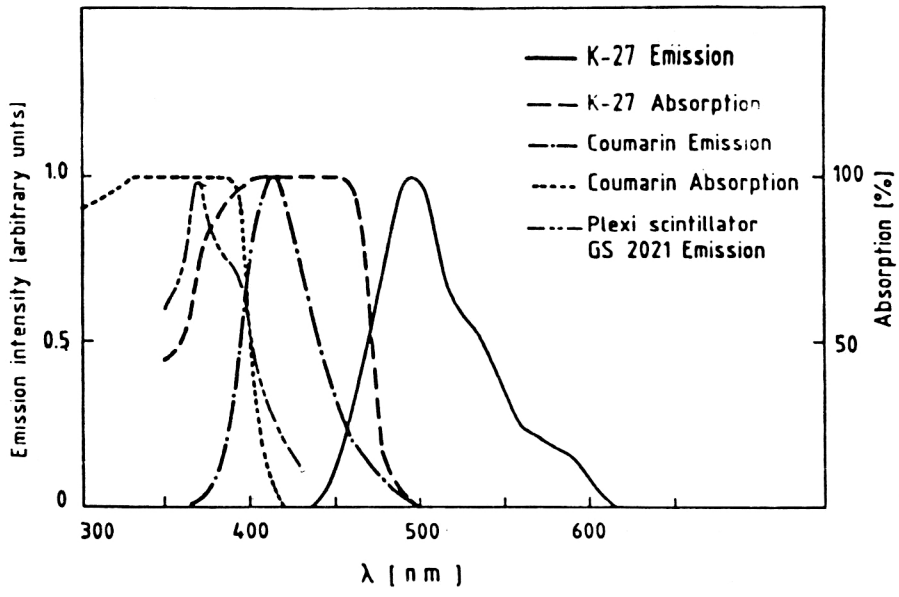

FIG. 4. Absorption and emission spectra of the fluorescence converters K-27 and coumarin, and emission spectrum of GS 2021 scintillator (Ref. 32).

cathode at 560 nm is about 6%. Completely satisfactory uniformity of the light collection as a function of distance to the fibers was obtained. Configurations where the fiber is laid in the face in the form of the letters U (Fig. 5d) and σ (Fig. 5e) are also used.[37] The latter makes it possible to decrease the number of photomultipliers by a factor of two, although the U-configuration is somewhat better regarding the uniformity of the light collection. When a mirror reflector was located at the end of a fiber of diameter 1 mm and length 4 m most distant from the photodevice, the light yield for the σ configuration was 84% of that for the U configuration. The characteristics of scintillation detectors with various configurations of fiber placement are described in more detail in Sec. 4.

As noted above, the BBQ shifter is widely used. The main component of its emission has a decay time of $\tau_1=18$ nsec, but there is a significant of the component with $\tau_2=620$ nsec (Ref. 38). According to the data of Ref. 39, 5% of the light is emitted during 0.5 μsec, which considerably limits the speed of response of the detector. For this reason the authors of Ref. 39 rejected BBQ as the WLS in favor of POPOP (0.01%), eliminating this typical impurity from the scintillator (PMMA+15% naphthalene and 1% butyl-PBD). In this scintillator $\Lambda_0=64$ cm.

K-27 ($\tau=10$ nsec) and pyrazoline (more precisely, 1,5-diphenyl-3-styryl-pyrazoline) are faster shifters than BBQ. The latter emits light with $\tau=5$ nsec at $\lambda_{max}=455$ nm (Ref. 40). Pyrazoline was applied to the surface of the light guide by immersing it in a solution. The typical light attenuation length was 1.5 cm, and the efficiency is of order 70% compared to that obtained using a volume WLS like BBQ.

A standard scintillator of the type SCSN38 (polystyrene+1% b-PBD+0.02% bis-MSB) with emission peak at 430 nm is used in many detectors. Such a scintillator is well matched to a shifter of the Y7 type (Kyowa Gas Chim. Co.), which emits light at $\lambda_{max}=490$ nm (see Fig. 6; Ref. 41). The light yield from the Y7 shifter proved to be 65% higher than when BBQ was used.

The laser dye #471 (Exciton Inc., USA) has roughly the same emission spectrum.

Among the currently most popular shifters is 3HF (3-hydroxyflavone), which is distinguished by its relatively short luminescence time ($\tau=6$ nsec) and large Stokes shift, the shift between the absorption and emission spectra needed for minimal absorption of the intrinsic light. The maxima of the absorption and emission spectra are respectively located at 350 and ~540 nm (Fig. 7; Ref. 43).

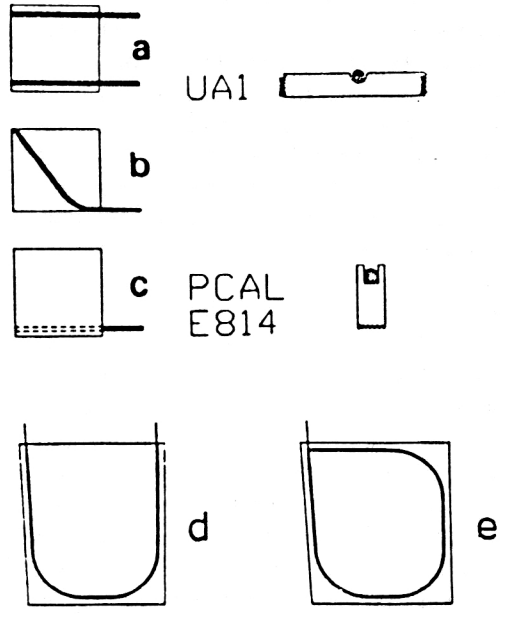

FIG. 5. Scintillation plates with spectrum-shifting fiber light guides.

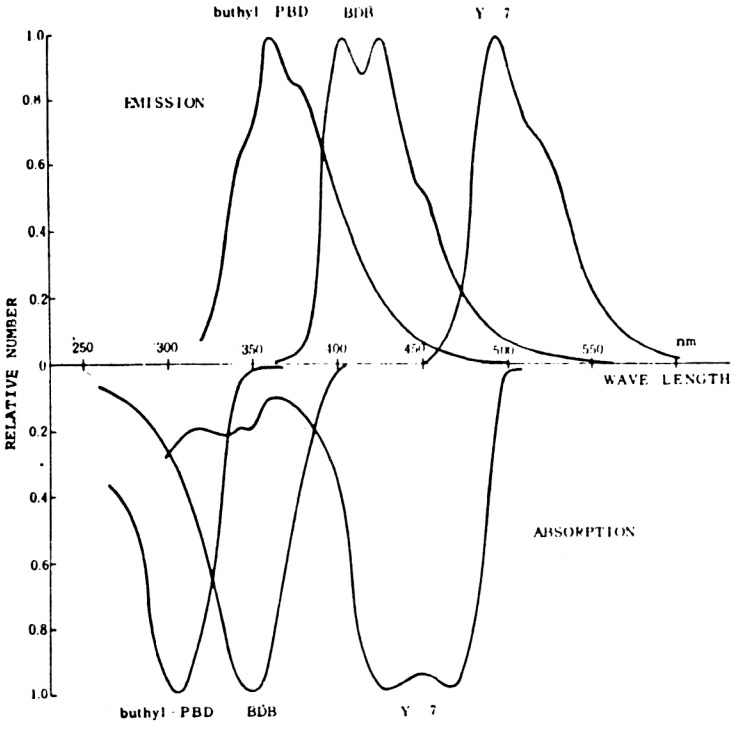

FIG. 6. Absorption and reemission spectra of the fluorescence converters b-PBD, BDB, and Y-7 (Ref. 41).

External influences affecting the light yield

Temperature degradation

As the temperature increases the light yield of a plastic scintillator decreases. The temperature coefficient is usually (0.1–0.4)%/1 °C. At high temperatures irreversible loss of the light yield occurs.

The effect of increasing temperature is manifested visually as a greenish-yellow coloring of originally blue scintillators. Partial absorption of the luminescence in materials of this coloring must tend to decrease the light yield. The density of greenish-yellow coloring is maximal at the surface and decreases inside the scintillator. Accordingly, the effect on the light yield varies with depth, as shown in Table III (Ref. 44).

We see that the light yield falls off beginning at the surface and continues to a depth of about 5 mm.

The decreased transparency of the material primarily affects the short-wavelength region of the scintillation light. For this region, scintillators whose emission spectrum is shifted from the blue to the green region are distinguished by high thermal stability.

The thermal stability of a scintillator depends on the basic material. According to the data of Ref. 45, in this respect polystyrene is superior to polymethacrylate and polyvinylxilole. The copolymer styrene with polymethylmethacrylate has high thermal stability. In a scintillator based on this copolymer the light yield at 120 °C first fell by 20%, and then remained constant for a relatively long time.

Aging

Does the light yield of a scintillator change under normal conditions, and if so, how much? To answer this question, the behavior of a scintillator made of styrene with additions of paraterphenyl and POPOP has been studied off and on for 9 years.[46] The scintillator had cross-section

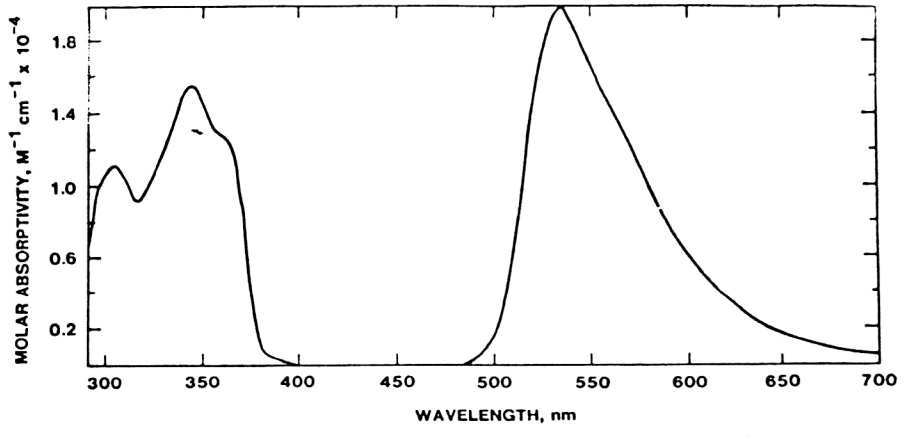

FIG. 7. Absorption and emission spectra of the fluorescence converter 3-HF (Ref. 43).

TABLE III. Relative light yield I of a polystyrene scintillator at various depths d after 1000 hours of being held at a temperature of 110–120 °C.

d, mm	0	2	3	5	7
I	0,2	0,4	0,5	0,9	1,0

dimensions 5×5 cm. The biggest change in the light yield was observed during the first few weeks after preparation of the scintillator and was ~6%. After 1–3 years the fall of the light yield decreased to ~1% per year. The luminescence time was practically unchanged. Other scintillators whose emission spectra are shifted toward the ultraviolet (400 and 394 nm) aged 5 to 10 times more rapidly. The aging occurred much more rapidly with increasing temperature. At 36 °C the light yield of a scintillator with $\lambda_{max}=400$ nm fell by 20%, and at 44 °C it fell by 40%.

The experimental results indicate that thermal-oxidation reactions occurring in the polymer base are the determining factor in the aging process. The products of these reactions are capable both of accentuating the excitation energy, which leads to actual extinction of luminescence, and of absorbing luminescence.

Naturally, the aging process begins at the surface of the scintillator in contact with the atmosphere. Under room conditions, as at higher temperature (see above), the action of the surrounding medium will grow with decreasing scintillator thickness. This is especially clearly manifested in film scintillators. Actually, in the thin ($X=10$ μm) counter discussed above, the light yield was decreased by 30% per year.[23] Thin scintillators of this type must be kept in a vacuum or in a nitrogen atmosphere.

Long-term measurements of the stability of the light yield have been made for an SCSN38 scintillator of dimensions 100×5×5 cm (Ref. 47). The light yields from two points of the scintillator located 10 and 50 cm from the end connected to a photomultiplier were compared. After 1000 days the light yield from the closest point had decreased by 0.4%, and that from the farthest had increased by 4.3%. The attenuation length, which in the original state was (81.8±1.7) cm, decreased by 8%. Another type of scintillator, SCSN81T2B, has $\Lambda_0=(196.2\pm13.1)$ cm and a light yield 20% higher than that of SCSN38. However, the changes in its characteristics after 1000 days were larger. The light yield was decreased by 1.9% for the closest point and 7.3% for the farthest. Λ_0 decreased by 13.5%. The large change of Λ_0 compared to the light yield indicates that the absorption of luminescence grows with time more rapidly than its actual extinction.

The effect of a magnetic field

The light yield of a scintillator increases slightly in a magnetic field,[48–52] and the effect of the field on the scintillator depends on the scintillator base material. In an acrylic scintillator a 1% increase in the light yield is observed already at 10^{-3} T, a 5% increase is observed at 10^{-2} T, and a 7% one at 0.2 T (Ref. 51). For a scintillator of thickness 10 mm based on PMMA, an increase of the light yield by 4.5% at 0.1 T is reported, along with a 2% increase for a scintillator of thickness 2 mm (Ref. 52). The scintillator light yield is affected beginning at a magnetic field strength of order 0.01 T.

The magnetic field sensitivity of scintillators based on polystyrene and polyvinyltoluene is 4 to 5 times lower.[53] In Table IV we give the results of measurements of the pulse height for a counter with an SCSN38 polystyrene scintillator of dimensions 203×199×2.5 mm as the field strength is raised to $B=1.4$ T (Ref. 54). The measurements were made in a 6-GeV electron beam. The systematic error of measuring B and the pulse height was 0.25%. The results of measurements at an electron energy of 2 GeV were similar. The effect of the magnetic field on the light yield of the scintillator proved to be independent of the direction of the field.

No change of the light yield in a magnetic field was observed when the scintillator was exposed not to radiation, but to ultraviolet light, which can stimulate the emission of light from the scintillator. A magnetic field also did not affect WLSs, in which the light emission occurs as a result of excitation by light of shorter wavelength and not by radiation.

Therefore, experiment indicates that the effect of a magnetic field on the light yield depends on the type of base material the scintillator is made from when the scintillator is exposed to radiation, and that there is no sensitivity to a magnetic field when short-wavelength light is detected. This suggests that a magnetic field affects the excitation or deexcitation of molecules of the base material and the transformation of energy from these molecules to the primary fluorescing impurities.[52]

TABLE IV. Relative variation of the pulse height U in the presence of a magnetic field B.

$B(T)$	0,0006	0,001	0,02	0,03	0,05	0,075	0,1	0,2
U,%	0,90	1,05	0,97	0,94	1,04	1,08	1,15	2,2
$\pm\sigma_{stat.}$	0,08	0,08	0,08	0,08	0,08	0,08	0,08	0,08
$B(T)$	0,3	0,4	0,5	0,6	0,8	1,0	1,2	1,4
U,%	3,08	3,66	4,10	4,64	5,85	6,75	7,78	8,71
$\pm\sigma_{stat.}$	0,08	0,08	0,09	0,09	0,09	0,09	0,09	0,09

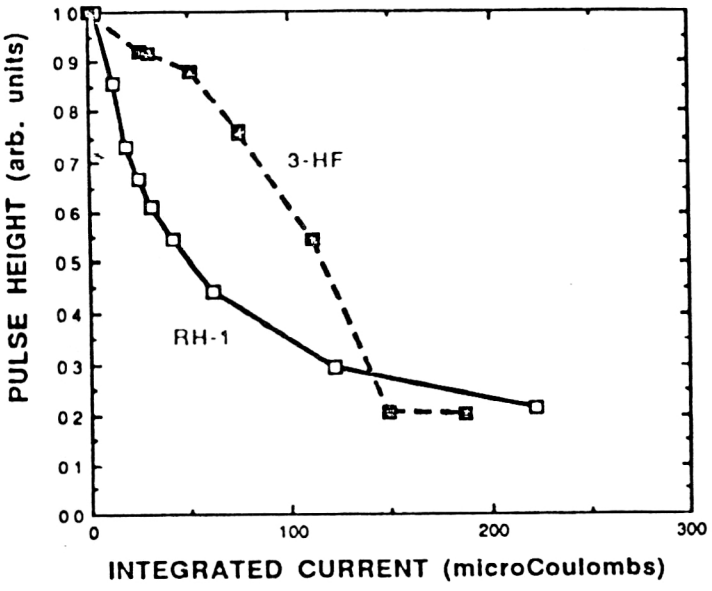

FIG. 8. Variation of the light yield as a function of the dose for scintillators with the fluorescence converters RH-1 and 3-HF (Ref. 73).

The effect of radiation

References 55–77 are devoted to the radiation strength of plastic scintillators.

The scintillator light yield is decreased by the destruction of emission centers as a result of radiation damage to the fluorescent material. However, this is not the only reason for the decrease. Loss of light due to radiation is mainly due to the formation of light centers in unimolecular rearrangements of the dyes introduced into the scintillator, and/or radiation-induced reactions with the plastic itself.[66] In the scintillators most widely used the light yield is usually decreased beginning at a dose of about 0.3 Mrad from ^{60}Co, and after 6 Mrad it amounts to 25–30% of the original yield.[63] The study cited reports that the light yield is restored to nearly its original value over the course of 10 days. For an SCSN38 scintillator based on polystyrene a 30% decrease of the light yield was observed after a 1.1 Mrad dose if a spot located 10 cm from the surface closest to the photomultiplier was irradiated.[47] The decrease rose by a factor of two when the irradiated spot was moved 50 cm farther away. This suggests that the light attenuation length Λ_0 of the SCSN38 scintillator is more susceptible to the effect of radiation than the amount of emitted light, which is determined by the conversion efficiency of the scintillator. The behavior of the scintillator in this respect is similar to aging (see above).

The surrounding medium affects the behavior of the scintillator characteristics in the presence of radiation. In particular, at a temperature of 50 °C in an argon atmosphere provided to hasten the recovery from radiation damage, scintillators have displayed a significant resistance to radiation.[58]

According to Ref. 65, for a base material of polystyrene and polyvinyltoluene, radiation-induced losses of the scintillator light yield are primarily the result of a decrease in the transport capability of the plastic at wavelengths in the fluorescent emission range. A loss of 38% over 1 cm has been observed in such scintillators at $\lambda=425$ nm after irradiation with a 3 Mrad dose. Meanwhile, in a scintillator based on polydimethyldiphenylsiloxane the losses were less than 1% after bombardment by a 18-Mrad dose in an argon atmosphere.

A scintillator based on polymethylphenylsiloxane with the fluorescents DMT (0.35%)+OLIGO415 (0.01%) (OLIGO stands for oligophenylene) retained its light yield up to 1 Mrad (Ref. 64). Here the decrease was 1–2%, while it was 40% in a standard scintillator of the type BC408. The initial light yield of this scintillator was 45% of that of BC408, and $\lambda_{max}=415$ nm (a "blue" scintillator). The authors of Ref. 66 reported the retention of the light yield at up to 16.5 Mrad in an argon atmosphere for a scintillator in which the primary fluorescent is OLIGO374A (4×10^{-3} moles/l) and the secondary is 1,1,4,4-tetraphenylbutadiene (2×10^{-3} moles/l), shifting the emission spectrum to $\lambda_{max}=460$ nm. Compared to BC408, the light yield of this scintillator is 25%, and its luminescence time is $\tau=1.76$ nsec.

Among the blue scintillators with greatest radiation hardness is Bicron RH-1 (Ref. 73). After bombardment with a 1-Mrad dose the light yield of this scintillator was completely restored in 22 days.[72]

A strong initial absorption in the short-wavelength region is characteristic of blue scintillators. This is also enhanced by thermal degradation.[67] Green and yellow scintillators lose their transparency more slowly. A steep falloff of the transparency to the level of blue scintillators and even below is observed in them only at large doses (see Fig. 8; Ref. 73).

The green scintillator with fluorescents DAT (di-*t*-amyl-*p*-terphenyl, $\lambda_{max}=375$ nm)+3HF ($\lambda_{max}=540$ nm; see Fig. 7) is remarkable. Under room conditions this scintillator withstood a dose of 10 Mrad, and its light yield was restored to the original value in 25 days.[68] This "annealing" process was shortened to one week by placing the sample (of cross section 2.2×1 cm) in an oxygen atmosphere with pressure 40 psig.

The properties of a polystyrene scintillator with only 3HF as a dopant have been studied and compared to a

standard scintillator with two fluorescing impurities: 1% pT+(0.01–0.1)% 3HF (Refs. 74 and 75). For a 1% concentration of 3HF in the first of these the light yield became the same as in the second, and after irradiation with a dose of 10 Mrad it decreased by only 3%. In such a scintillator the excitation of polymeric molecules is transmitted to the single fluor at distances measured in Angstroms, and a shift of waves from 320 nm directly to the green region with a luminescence time of 8.53 nsec occurs. It is observed that radiation-induced color centers do not strongly affect the transmission mechanism operating at such short distances. However, in extended scintillators losses in transmission can prove more important than loss of the light yield, and for such cases the authors tend to prefer a scintillator with two fluorescents.

The radiation hardness of scintillators with 3HF is also noted in Ref. 76, in which the results of studies of a broad class of scintillators are reported. Naphthalene-containing materials like X25 (naphthalic anhydride derivative) and X31 (naphthalimide derivative) are also recommended for use as the secondary fluor. The light yield is not greatly changed after irradiation with a 10-Mrad dose for all three types of scintillator, but it is considerably lower for the scintillator with 3HF before irradiation.

An increase of the radiation hardness was also observed after the introduction of naphthalene N into a scintillator based on PMMA, which is considered to be rather sensitive to radiation.[77] For example, PMMA+15% N+0.4% POPOP was more resistant to radiation than a polystyrene scintillator with the addition of 2% pT+0.1% POPOP.

Slight damage and nearly complete restoration were observed when the fluorescents OLIGO 408+0.02% K27 were used.[69] In scintillation fibers made of this scintillator the light yield after a 10-Mrad dose was decreased by up to 60% and restored by up to 90% after 13 days, during 10 of which the scintillator was in oxygen and during 3 of which it was in air.

Radiation produces two types of damage centers: annealable and nonannealable ones. The annealing rate under room conditions is much lower than in an oxygen medium. However, the rate of annealing in air grows with temperature, and at 80 °C it is slightly higher than the rate in oxygen.[71] It is not yet completely clear how the radiation damage depends on the rate at which the dose is accumulated. For example, in acrylic scintillators a radiation dose accumulated at a slow rate produced considerably more damage than when the rate was high.[56] However, as shown in Ref. 59, polystyrene scintillators do not display any significant dependence on the rate at which the dose is accumulated.

Scintillators based on elastometric polymers display the highest radiation hardness.[70] In creating such a polymer the initial idea was that a color center induces stress in a vitreous polymer. Therefore, the chemical structure of polystyrene and PMMA was modified so as to lower their transition temperatures for vitrification to below room temperature. This resulted in a scintillator whose light yield remained constant to within ±10% under irradiation with a 20-Mrad dose. The light yield of the scintillator is comparable to that of a polystyrene scintillator, but the light attenuation length (Λ_0=0.5 m) is still considerably smaller.

3. SPECTROMETRY OF CHARGED PARTICLES OF INTERMEDIATE AND LOW ENERGY

Plastic scintillators can be used as absorbers of charged particles for measuring their energies in the range of tens and hundreds of megaelectronvolts. The lower limit arises from the decrease of the scintillation efficiency at high ionization density. In this respect organic scintillators are greatly inferior to inorganic scintillating crystals. The pulse heights of a detector using a plastic scintillator for detecting, for example, α and β particles with energy 5 MeV differ by 5 to 10 times. However, for protons and pions, which are lighter than α particles, plastic scintillators are completely applicable for spectrometric measurements beginning at ~10 MeV and higher. At this proton energy the loss of scintillation efficiency owing to high ionization density is about 40%.

For thick scintillators the pulse height is affected by nuclear interactions between the detected particle and the scintillator material. For example, for protons of energy 100–700 MeV the number of inelastic interactions is ~1% in 1 g/cm^2. Most of these pertain to processes of "star production," especially at lower energies.

Stars contain short-ranged charged fragments with high ionization density and also neutral fragments. If the scintillator thickness is considerably smaller than the particle range, then each star-production event will, as a rule, be accompanied by an increase of the light burst owing to strong ionization by short-ranged fragments. However, if the particle range falls mainly in the bulk of the scintillator, then, conversely, in star production the light burst weakens in the flight of the particle. This phenomenon is due to the decrease in the scintillation efficiency at high density of ionization from the short-ranged charged fragments of the star, and also because some fraction of the energy is carried by neutral fragments. As a result, in the ionization-loss spectrum there appears a tail extending to lower values from the total absorption peak.

For energy depositions of tens of MeV and above the number of photoelectrons is usually completely sufficient to obtain a peak width at half-max (FWHM) of about one percent. However, in practice the resolution can worsen to ten percent and more owing to nonuniformity of the light collection. The dependence of the collection coefficient on where the scintillation is formed can be taken into account by a coordinate device such as a proportional chamber (PC). Of course, scintillation spectrometers have worse resolution than semiconductor or magnetic spectrometers. However, for a number of experiments their resolution is completely satisfactory, and their high speed of response and relatively low cost when used as the basis of wide-aperature setups are attractive features. In such setups particle identification is performed using the results of measuring the energy and ionization losses and/or the particle time of flight.[78–82] A relatively high energy resolution was

obtained using a PC to determine the coordinates of the point where particles entered the scintillator.[78] The energy spectrum of 50-MeV pions had FWHM=4%, and that of 70-MeV protons had FWHM=3%. Of those referred to above, the setup described in Ref. 79 with 4π geometry had the largest range of measured energies, 30–750 MeV. It contained a liquid in addition to a plastic scintillator, which made it easier to have a large volume.

The spectrometer discussed in Ref. 83 was designed for protons of energy 3–200 MeV. In it ($\Delta E-E$) scintillators serve simultaneously as the walls of an extended cavity which can be filled with a gas at a pressure of up to 5 atm acting as the target, or it can have a thin solid target placed inside. The same maximum energies are measured by the LBL spectrometer made in the form of a sphere.[84] It is constructed of 815 ($\Delta E-E$) telescopes and 176 time-of-flight telescopes, covering a solid angle of 97% of π.

Phoswich counters

A distinctive feature of the last two spectrometers[83,84] is the use of ($\Delta E-E$) telescopes in the form of a structure called a "phoswich detector." In such a detector the ΔE and E scintillators are opticaly joined and connected to the same photomultiplier, while the scintillators have different luminescence times.[85,86] This makes it possible to discriminate a signal according to the shape of the pulse. In both spectrometers a plastic is used for the thick scintillator. CsI(Tl) with a luminescence time of ~ 1 μsec is used as the thin scintillator in Ref. 83. Its thickness varied from several hundred micrometers to 12 mm, depending on the requirements of the experiment. CsI(Tl) ensures a linear dependence on the proton energy, beginning at about 3 MeV. The phoswich structure has made the good experimental separation of protons and pions possible.

In the LBL Plastic Ball detector the ΔE detectors are made of CaF_2(Eu), the luminescence time of which is also 1 μsec. This crystal is 4 mm thick, and the second one, a plastic, is 32 cm thick. An individual module is made in the form of a triangular prism with a base on which the diameter of the photocathode is inscribed. The spectrometer has performed good separation of pions, protons, deuterons, ^{3}He, and ^{4}He.

A phoswich detector of similar composition, namely, CaF_2(Eu) and a plastic scintillator (NE-110), is considered in Ref. 87, and a liquid scintillator (NE-213) was used in Ref. 88.

A phoswich detector is designed for the same purpose as a ($\Delta E-E$) telescope, in which the ΔE detector or both detectors are semiconductor detectors. Although phoswich detectors are inferior to the latter in energy resolution, they provide a less expensive realization of the structure needed for experiments. In both versions the thickness of the first, thin detector imposes a limit on the minimum measurable energy. This factor is particularly manifested in the identification and measurement of the energy of short-ranged particles like heavy ions. Here preference is usually given to a thin detector whose thickness can be minimized (in g/cm^2) and its area maximized. It is easier to solve this problem using plastics than using semiconductors. In addition, a plastic scintillator can give a very fast start signal. The second, thick detector is naturally chosen to have larger luminescence time. For example, the authors of Ref. 89 describe a combination of an NE102A plastic scintillator ($\tau=2.4$ nsec) of thickness 200 μm and a CsI(Tl) scintillator of thickness 50 mm. Such a phoswich detector has satisfactorily identified products of nuclear reactions of ^{40}Ar (30 MeV/nucleon) on a carbon-deuterium target with charge up to $z=19$.

Both scintillators in a phoswich detector can be plastic ones, since fast and slow plastic scintillators are available. In particular, the scintillator NE115 has a luminescence time of 350 nsec. The combination NE102A+NE115 is quite suitable for the construction of a phoswich detector.[90] The two scintillators were pressed together by the heat-press technique and combined to form a single one.[91] The thickness of the thin scintillator was 1 mm, and the total thickness was 5 cm. The area of an individual phoswich detector was 6.5×6.5 cm. A multidetector system was created using 32 such detectors. The pulse heights from each photomultiplier were analyzed using two channels controlled by gate signals of different duration, 30 and 400 nsec. The first channel passed short pulses from the fast scintillations of the thin scintillator, and the second recorded slow scintillations. The system was able to separate isotopes with $z=1--9$ for $E<30$ MeV/nucleon.

A phoswich detector which was similar except for being thicker (the first scintillator was 2 mm thick and the second was 30 cm thick) made it possible to extend the proton detection range to 200 MeV (Ref. 92). 120 such crystals were used to construct a wall covering the angular range between $\theta=10°$ and $\theta=30°$ for $\phi=0$–360°. This wall served as an auxiliary to a sphere of BaF_2 crystals for creating a 4π system (MEDEA) designed for exclusive measurements of heavy ion collisions at intermediate energies.

Plastic scintillators of a different type, Bicron BC-400 ($\tau=12$ nsec) and BC-444 ($\tau=450$ nsec), were used in Ref. 93. The thickness of the fast plastic was chosen to lie in the range 60–400 μm. A "dwarf ball" of inner radius 43.2 mm and typical cell thickness of 6.25 mm was constructed of 72 phoswich detectors. However, better characteristics were obtained when the BC-444 was replaced by CsI(Tl) (Ref. 94). The crystals were hexahedrons. For angles greater than 40° the thickness of the thin plastic scintillator was 10–30 μm. The technique of preparing these film scintillators is described in Ref. 95.

An optical feature of such thin scintillators is the shift of their light-emission spectrum to the ultraviolet. Whereas for a thick plastic $\lambda_{max}=420$ nm, in a film scintillator the maximum of the emission spectrum is shifted to 380 nm. The reason for this is that the thickness quoted is insufficient for the effective capture of light from the primary fluorescent by the secondary, which reemits light near $\lambda_{max}=420$ nm.

Phoswich detectors of BC-400 and CsI(Tl) were used to construct spheres for $\theta=32$–168°, and, in the range $\theta=4$–32°, a wall composed of forty modules. In nuclear reactions using an ion beam of energy 10 MeV/nucleon it

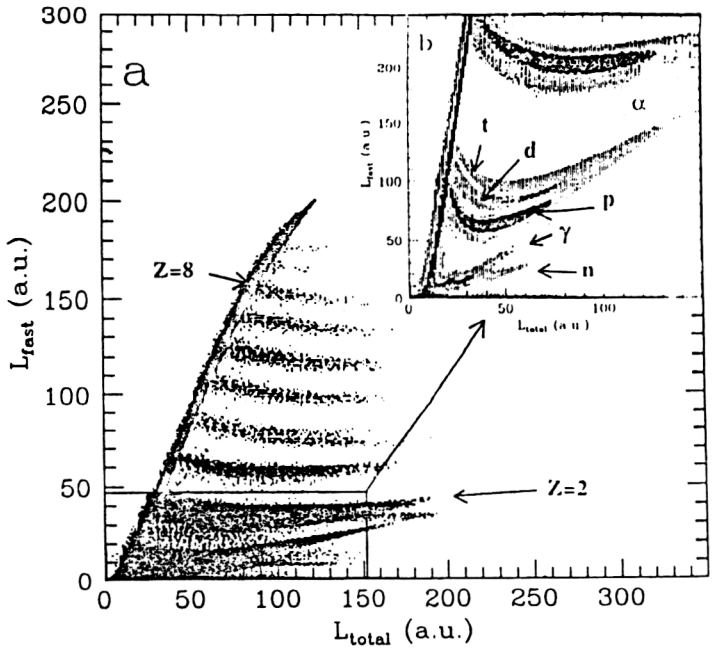

FIG. 9. Two-dimensional spectrum (a) of the light yield of a phoswich detector with BaF_2 for the fast component as a function of the total light yield obtained in the reaction $^{40}Ar+^{27}Al$ at $E_L=26$ MeV/n; (b) magnified view of the boxed region (Ref. 100).

was possible to identify ions with charge up to $z=25$, beginning with $^{1,2,3}H$ and $^{3,4}He$. A different version of the miniball (MSU) was made of 188 phoswich detectors forming 11 rings coaxially positioned around the beam axis.[96] As in the preceding system, scintillating plastic film (40 μm) and 2-cm-thick CsI(Tl) were used. It is noteworthy that the phoswich detectors operated in a vacuum.

In those cases where the counting rate is important, the plastic scintillator BC-444 is preferable to CsI(Tl). The authors of Ref. 97 give for BC-444 the luminescence time $\tau=187$ nsec (260 nsec in Refs. 98 and 175) and a light yield of 41% relative to that of anthracene. The distinctive feature in Ref. 97 is the large area (12×12 cm) of the thin (0.7 mm) fast scintilator BC-408. The fast and slow scintillators were joined by heating and pressure. The nonuniformity of the thin counter was less than 3%. A setup consisting of 32 such phoswich detectors of trapezoidal form was built for studying reactions in the range 10–40 MeV nucleon.

The advantage of CsI(Tl) is the significantly weaker dependence of the light yield on the ionization density than in a plastic scintillator, which is especially important for the absorption of relatively short-ranged particles in a thick scintillator. However, the large luminescence time of the crystal significantly restricts the speed of response of the setup. For this reason, the authors of Ref. 98 gave preference to nonactivated cesium iodide, which has a short luminescence time (less than 30 nsec), even though the light yield of such a crystal is an order of magnitude lower than that of the activated one. The dimensions of the CsI were 10×10×5 cm, and it was placed behind a slow plastic scintillator of the BC-444 type of thickness 3 mm. For measuring the total light yield using such a phoswich detector a time interval of 1 μsec was chosen, with 100 nsec for the fast component. Its fraction for CsI was 60%, while for the plastic it was only 26%. The detector separated protons, deuterons, tritons, and ^3He and ^4He nuclei with energies below 200 MeV.

The phoswich detector made of a fast, thin plastic and a BaF_2 crystal, which has two luminescent components $\tau_1=0.6$–0.8 nsec and $\tau_2=620$ nsec with respective intensities of 5% and 16% relative to the light yield of NaI(Tl), has interesting properties. The typical light yield of the plastic is ~25%, i.e., not much higher than the total light yield of BaF_2. In Ref. 99 a phoswich detector was made of 260-μm-thick NE102A plastic and 10-cm-thick BaF_2 for the simultaneous detection and identification of light charged particles and heavy ions with $z=1$ to $z=18$. Additional time-of-flight information was used to separate isotopes with $z=1$. The measurements were performed in a ^{40}Ar beam of energy 27 MeV/nucleon. A combination of these types of scintillator in the form of a hexagonal prism of area 37 cm^2 and depth 15 cm is described in Ref. 100. The operation of this detector was studied for two thicknesses of the plastic, 50 μm and 1 mm, by detecting the products of the reaction $^{40}Ar+^{27}Al$ in a beam of argon ions of energy 26 MeV/nucleon. The fast part of the pulse from the photomultiplier had a rise time of several nanoseconds and a fall time of ~15 nsec. It is due to both the plastic and the BaF_2 if the charged particles penetrated inside this crystal, and only to BaF_2 in the conversion of gamma quanta or neutrons in this crystal. These forms of neutral radiation are observed along with charged particles, which is a typical feature of this type of phoswich. In Fig. 9 we show a two-dimensional spectrum in which the light yield from the fast component and the total light yield are plotted along the axes. Here the pulses from the photomultiplier respectively passed through 50-nsec and 1.5-μsec gates. The initial part of the spectrum is shown separately on a magnified scale, so that the separation of charged particles, neutrons, and gamma quanta of low en-

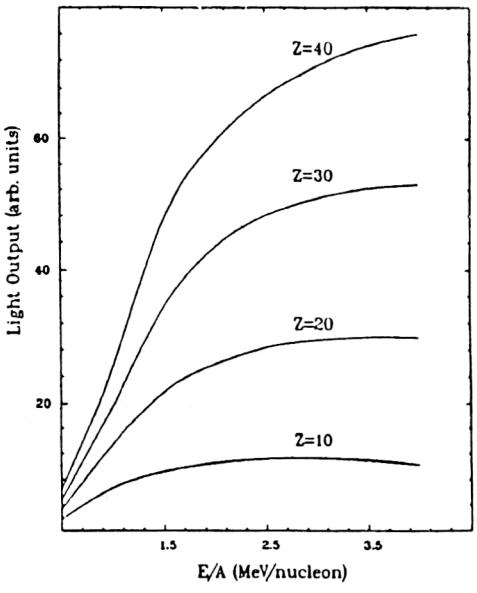

FIG. 10. Light yield of a plastic scintillator of thickness 10 μm for heavy ions with various z and E/A (Ref. 101).

ergy can be demonstrated more clearly. However, for a plastic thickness of 1 mm the threshold for producing the two-dimensional spectrum is rather high: 16.1 MeV/nucleon for ^{16}C. A thickness of 50 μm proved insufficient for obtaining the needed light burst using a plastic scintillator from protons, in order to separate them from neutral radiation. As a compromise, a thickness of 100–200 μm was chosen.

Detection of low-energy ions and electrons

The silicon detector is the traditional spectrometric device for ions with an energy of several MeV. However, at large counting rates use of a scintillation detector may be preferable, especially if the ion time of flight is to be measured along with the energy. In particular, such a technique has been used to detect ions with energy below 4 MeV/nucleon in the range up to $z=40$ (Ref. 101). The scintillator was applied in the form of a 10-μm-thick film on the photocathode of a photomultiplier. For ions of these energies the light yield in the first approximation depended linearly on z (Fig. 10). The distribution of products of the reaction $^{32}S+^{27}Al$ at 142 MeV was measured at small angles. The results were similar to those obtained earlier using a silicon detector.

Electrons, which are very light, undergo strong multiple scattering in matter. For this reason the thickness of the matter in which electrons are absorbed is considerably lower than their total mean free path R_0, and the difference between R_0 and the experimental mean free path grows with increasing atomic number Z of the material. The experimental mean free path of electrons of energy 0.2–3.0 MeV in plastic is $\sim 0.9R_0$, while in NaI it is about $0.5R_0$.

Electrons also undergo isolated, single scatterings in which their direction of motion is reversed, i.e., back reflection (albedo) arises. This occurs with decreasing electron energy and increasing Z, as illustrated in Table V.

The closest data for a plastic scintillator are those from the first column, while for sodium and cesium iodides the closest data are those from the fourth column. The coefficient of reflection from these inorganic crystals is very high, while in the case of plastic it is less than 1%. However, for $E<4$ MeV it is impossible to neglect reflection on the plastic, especially if the electrons do not hit it at perpendicular incidence. This can be seen from Table VI.

For example, if for perpendicular incidence of 1-MeV electrons the number of reflections is 4%, a slope of the electron trajectory relative to the scintillator surface of 60° will be accompanied by the reflection of almost one fourth of them.

Pion detectors

In a number of experiments at accelerators medium-energy charged particle accelerators it is necessary to use relatively small detectors with good energy resolution. References 106–108 describe total-absorption detectors of pions with energies of up to 100 MeV which possess an energy resolution of FWHM = 1–1.5 MeV for positive particles. In all these detectors the particles enter a thick scintillator from the end farthest from the photocathode. The particle trajectory points along the photomultiplier axis, which makes it possible to minimize the effect of a longitudinal nonuniformity of the light collection in the scintillator. A scintillator length of 25 cm is sufficient for the absorption of 100-MeV pions. Their separation from protons is accomplished by either the addition of a ΔE detector[106,107] or the time-of-flight technique.[108] In stopping in the scintillator a positive pion decays according to the scheme

TABLE V. Coefficients of electron back scattering (Refs. 102 and 103).

E, meV \ Z	6	13	29	47	73	92
4	0,0080	0,033	0,110	0,187	0,275	0,306
6	0,0055	0,018	0,073	0,134	0,208	0,237
8	0,0045	0,014	0,050	0,096	0,160	0,183
10,2	0,0036	0,011	0,038	0,074	0,125	0,141
12	0,0030	0,009	0,030	0,061	0,095	0,116

TABLE VI. Coefficient of electron back scattering at various angles of incidence θ for matter with $Z=7.2$ (Refs. 103–105).

θ° \ E, meV	3	2	1	0,6	0,4	0,2
0	0,02	0,03	0,04	0,050	0,060	0,070
30	0,05	0,07	0,08	0,085	0,090	0,095
45	0,08	0,10	0,12	0,125	0,130	0,135
60	0,16	0,20	0,23	0,240	0,245	0,250

$$\pi^+ \to \mu^+ + \nu, \quad \tau_{\pi^+} = 26.04 \text{ nsec};$$

$$\mu^+ \to e^+ + \tilde{\nu} + \nu, \quad \tau_{\mu^+} = 2.198 \ \mu\text{sec}.$$

The muon emitted in the pion decay has energy equal to 4.13 MeV, and the energy of the positron produced in the muon decay varies from 0 to 53 MeV.

Therefore, three signals appear at the photomultiplier output. The first of them, proportional to the π^+ energy, appears at the instant the π^+ hits the scintillator. The second signal, with a small but standard height proportional to 4.13 MeV, appears after a certain delay, determined by τ_π. The third signal appears after an even larger delay determined by τ_μ, and its height is relatively large and uncertain. The second signal can be used as the sign of the decay of a positive pion. For this it is detected within some range Δt which is not so large that the probability of detecting the third signal distorting the standard amplitude would remain small. The optimum proved to be $\Delta t = 117$ nsec, which corresponded to a detection efficiency of 95%. However, also for this Δt the error introduced by the third signal could not be neglected.

In analyzing the spectra measured in total-absorption detectors it is also necessary to take into account the distortions due to nuclear interactions of pions with the scintillator material. The spectrum corrections can be made using special calibration measurements. For example, in Ref. 108 the spectrometric information was read out by an independent time-of-flight system simultaneously with the determination of the energy by a total-absorption detector. A value FWHM = 1.7 MeV was obtained for a resolution of 0.5 MeV, a time-of-flight base of 1 m, and a pion energy of 20 MeV. It is noteworthy that nuclear interactions do not affect the measurement of the time, so that it becomes possible to introduce the corresponding correction into the total-absorption energy spectra.

In addition to a total-absorption detector for measuring the particle energy and also for particle identification, a range telescope consisting of a set of thin scintillation plates located one behind the other can be used. Such telescopes have been used, in particular, to study pion production in collisions of heavy ions of intermediate energy.[109] The thicknesses of the scintillation plates and mean free paths of pions stopped in the corresponding plates are given in Table VII.

The first four counters in the telescope are mainly used for discrimination of the intense proton background. Scintillators Nos. 5–10 are the elements in which pions of energy from 27 to 82 MeV stopped in them are detected. Scintillators Nos. 11 and 12 with a copper absorber between them are introduced for counting high-energy pions. Since they are heavier, protons have larger ionization losses in scintillators than do pions with the same mean free path. As a result, these particles are easily separated. Signals from μ^+ are also used for π^+ identification, whereas only ΔE signals are used for π^-. Here roughly 5% of cases with false stopping structure are discarded. This structure occurs if the π^- at the end of its path captures and emits a secondary particle, which is stopped in the next scintillator.

4. CALORIMETERS

In the detector considered above the total thickness of the scintillators absorbing pions with energy up to 100 MeV was 30 cm. The realization of the absorption of pions and other hadrons of higher energy in a "pure" scintillator is technically difficult or even impossible. The nuclear absorption length in a plastic scintillator is ~ 80 cm. As is well known, this is the length of the mean free path between nuclear collisions for high-energy hadrons.[110] This usually pertains to heavy particles such as protons, and for pions this length is one and a half times larger.

A large decrease in the detector dimensions can be achieved by alternating layers of scintillator with denser "passive" matter, for example, copper and iron. In particular, this method was used to construct an efficient detector of neutrons with energies of hundreds of MeV.[111] Then

TABLE VII. Structure of the range telescope. № is the order number of the scintillation plate, X is its thickness, and E is the average energy of a pion stopped in it.

№	1	2	3	4	5	6	7	8	9	10	11	Absorber	12
X, mm	5	5	10	15	25	30	30	30	30	30	10	20 (Cu)	10
E, meV					32	43	52	61	70	78			

a study appeared describing a total-absorption detector of similar configuration, but with ionization chambers instead of scintillators.[112] This device is referred to as a calorimeter, since the particle energy absorbed in it is ultimately transformed into heat. The amount of this heat is proportional to the total ionization induced by the primary and all the secondary particles arising in inelastic interactions. Later, scintillators were most often the preferred material for use as a detecting medium. Since it is a denser medium, a scintillator ensures a larger value of the measured ionization losses and, consequently, smaller fluctuations in them.

In the calorimetry of electromagnetic radiation (gamma quanta, electrons, and positrons of high energy) the standard passive material is lead, which has a small radiation length (the length of the path over which the primary beam is attenuated by a factor of e). Lead-scintillator sandwiches[113–115] have become widely used owing to their relatively low cost and high speed of response. The use of a WLS for light collection from a set of scintillation plates has considerably simplified the construction of such detectors and made them less expensive (see, for example, Refs. 116, 117, and 33). However, sandwich calorimeters are greatly inferior in energy resolution to electromagnetic calorimeters constructed on inorganic scintillating single crystals (see Ref. 118, for example). The accuracy of energy measurement by a sandwich detector is mainly determined by the so-called sampling fluctuations due to the statistical nature of the distribution of the ionization loss between the layers of absorber and the detecting medium. Nonuniformity of the light collection from the relatively thin layers of the scintillator also tends to worsen the resolution.

In hadron calorimetry the main processes leading to absorption of the energy of the primary particle and its "descendents" are interactions with the production of nuclear-active particles, primarily pions. A significant part of the energy is transferred to π^0 mesons and then, as a result of their decay into gamma quanta, is transformed into the electromagnetic component. Iron and copper have a small enough radiation length to ensure the effective absorption of electromagnetic radiation, which is why they are widely used in calorimeters.[119–132]

The calorimeter length is chosen on the basis of the hadron-shower extent, which grows with energy. The length can be decreased by increasing the ratio of the thicknesses of the absorber and scintillator layers. However, here it becomes more and more difficult for the low-energy nuclear fragments and gamma quanta produced in inelastic interactions to reach the scintillator. For iron and scintillator thicknesses of, for example, 25 and 5 mm, respectively, the typical calorimeter length is 2 m. The nuclear interaction length in iron is 17.1 cm, and most of the hadron shower occurs at ~ 10 cm.

A deficiency of iron and copper calorimeters is the fact that the signal in the absorption of protons and charged pions (h) is smaller than in the absorption of electrons (e) of the same energy. The signal from neutral pions decaying into gamma quanta is the same as for electrons. The ratio of charged and neutral pions in showers fluctuates, which, owing to violation of the equation $e/h=1$, leads to corresponding fluctuations in the measured energy losses. Fluctuations of this type make a contribution in the form of a constant term in the dependence of the energy resolution on the hadron energy.[137]

The ratio $e/h=1$ can be obtained if uranium is used as the absorber.[133–143] This is related to the production, in nuclear interactions with ^{238}U, of neutrons, which in scintillators give a compensating contribution to the observed signal. Most neutrons come from the evaporation of highly excited nuclei, with smaller contributions from nuclear fission and spallation.[145] The typical neutron kinetic energy is 2 MeV, and the typical yield per 1 GeV of initial energy is 33 neutrons below 20 MeV.

The nuclear absorption length in uranium is 12 cm. The ratio $e/h=1$ is obtained when the thicknesses of the uranium and scintillator plates are nearly the same. For example, in the calorimeter of the ZEUS collaboration these thicknesses are respectively 3.2 and 3.0 mm (Ref. 138). The scintillator thickness was later decreased to 2.5 mm. For this calorimeter the quoted resolution is $\sigma/E = 35\%/\sqrt{E[\text{GeV}]} + 2\%$, measured for hadrons.[143]

However, as shown in Ref. 144, the ratio $e/h=1$ can be obtained not only using uranium absorbers. Processes involving neutron production also occur in lead, but there are fewer of them. Compensation should be expected for a ratio of the lead and scintillator of $\sim 4{:}1$, instead of the 1:1 for uranium. The same effective nuclear interaction length, about 20 cm, is obtained in both cases. The experimental value of e/h for energies above 10 GeV was 1.05 for lead and scintillator thicknesses of 10 and 2.5 mm, respectively.[145] The change to such thicknesses instead of equal ones[146] was accompanied by an improvement in the energy resolution by a factor of 1.2, which came to $44\%/\sqrt{E[\text{GeV}]}$. However, it is still inferior to that obtained with the uranium calorimeter.[138] According to Refs. 147 and 148, the dominant contribution to the energy resolution for such relatively thick lead layers comes from sampling fluctuations, while the intrinsic resolution for lead is almost two times better than for uranium. By intrinsic resolution we mean the limit arising from fluctuations of the shower itself due to the content of undetected secondary particles or fluctuating energy losses related to nuclear breakup.[147]

Decrease of the ratio of the lead and scintillator thicknesses to 3.3:1 accompanied by a decrease in the sampling flutuations led to an improvement of the resolution to $40\%/\sqrt{E[\text{GeV}]}$ (Ref. 37). The same ratio of the lead (1.0 cm) and scintillator (0.3 cm) thicknesses was reported in Ref. 149, in which the calorimeter was made of 59 such pairs, broken up into four sections in the longitudinal direction. The response of this calorimeter to low-energy pions, muons, and positrons, from 400 to 250 MeV/c, was studied. The calorimeter could even be used at lower energies; here the resolution varied within the range $\sigma=47$–17%.

Among the obvious advantages of lead are its low cost and ease of machining. Lead calorimeters are faster than

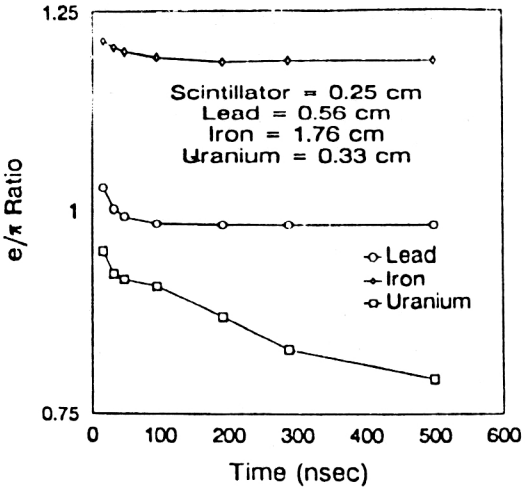

FIG. 11. The ratio e/π as a function of the integration time in scintillation counters using uranium, lead, and iron (Ref. 153).

uranium ones, which is especially important for use in the high-luminosity accelerators presently under construction.[150] In lead calorimeters the neutron energy is mainly loose owing to inelastic scattering on the hydrogen of the plastic and to the capture of slow neutrons by nuclei of the material, which results in the production of low-energy gamma quanta. The slowing of neutrons to thermal velocities and their subsequent capture is accompanied by the appearance of a tail after the fast (10 nsec) main part of the signal. However, for lead the contribution of this process is small, since the capture cross section for thermal neutrons is only 0.1 b, while for ^{238}U it is 2.7 b (Ref. 151). Whereas in a lead (or iron) calorimeter less than 1% of the energy is deposited between 50 and 100 nsec, in uranium nearly 10% of the energy is deposited in the interval 100–500 nsec (Ref. 152). In connection with this, it turns out that when uranium is used the ratio e/h depends strongly on the time of integration of the charge from the photomultipliers. This is illustrated in Fig. 11 (Ref. 153), in which we show the results of calculations for the three types of calorimeter. It should be noted that these calculations demonstrate that the optimal ratio of the lead and scintillator thicknesses is 2:1.

At the end of a shower a large number of slow particles are created which produce tracks with large ionization density. The latter tends to decrease the scintillation efficiency in accordance with the Birks formula (see Sec. 2), the denominator of which contains the parameter KB, which is given in Table VIII for a number of organic scintillators.[152]

Of the scintillators listed in this table, SCSN38 has the minimum KB parameter (0.85×10^{-2}), and for it the calculated ratio e/h is 4% smaller than for Pilot B, which has the largest KB parameter.[152] In the calculation the thickness of the lead plates was taken to be 5.6 mm, and that of the scintillator plates was 2.5 mm; the detected particles were 10-GeV pions.

A small KB parameter for SCSN38 was also obtained in Ref. 154, where the value 0.806 ± 0.012 is quoted, and for NE102A, where $KB=0.882\pm0.012$. Accurate measurements of the proton and electron energies were made to determine KB. Here it was assumed that for electrons the light yield is strictly proportional to their energy, which is not completely correct. The inclusion of the small deviation from linearity at very low electron energies leads to the following values of KB for SCSB38 and NE102A: 0.842 ± 0.015 and 0.921 ± 0.015, respectively.

Light collection in laminated calorimeters

The light from a large number of scintillation plates of a calorimeter is usually transported to photomultipliers via light guides containing WLSs (see Sec. 2). Light guides of various forms are used: blocks, plates, rods, fibers, and strips.

In Ref. 124 two rods were optically connected. One had a WLS of the type Yellow 323, and the other had BBQ, emitting green light. These rods respectively pass through the photon and hadron sections of the calorimeters. Light filters allow the yellow and green light to be separated before reaching the photomultipliers. However, it is more usual to transport the light from the photon and hadron sections along independent plates with a green WLS incorporated into the material of which the light guide is made.

Light guides with WLSs applied to their surface are described in Ref. 155. It is pointed out that an advantage of such a structure is that the sensitivity to Čerenkov light of a film WLS is smaller than that of a volume WLS. If the WLS is incorporated into the bulk of the light pipe there is effective shifting of the Čerenkov light produced in the passage of particles from electromagnetic and hadronic showers along the light guide. The Čerenkov signal can make up a significant fraction of the main signal of the scintillator-WLS system. This leads to the appearance of so-called "hot spots," in which the uniformity of the calorimeter and its energy resolution are sharply degraded owing to fluctuations of the number of particles inducing Čerenkov radiation.[156,157] To weaken this effect, impurities are introduced which absorb the short-wavelength part ($\lambda < 380$ nm). Naturally, along with the Čerenkov light, the

TABLE VIII. KB parameter for typical commercial scintillators.

Scintillator Type	NE102	NE213	Pilot B	Stilbene	Anthracene	NE230	SCSN38
KB-parameter$\times10^2$, $g\cdot cm^{-2}\cdot MeV^{-1}$	1.31	1.25	1.59	0.955	1.46	1.10	0.850

corresponding short-wavelength part of the scintillation burst is also lost. When film WLSs are used, it is possible to introduce into the volume impurities with absorption boundary at longer wavelengths, thereby reaching the beginning of the radiation band of the spectrum shifter without decreasing the efficiency of scintillation light absorption by a film WLS. This has made it possible to decrease the nonuniformity of the device by about a factor of two.[155]

The deposition of a WLS by means of immersion of the light guide in a solution makes it relatively easy to obtain the required variation of the WLS thickness along the light guide. In this way it is possible to compensate for the loss of the shifted light when it travels along the light guide. Measurements with a rod of diameter 19 mm showed that whereas the attenuation length was 1.3 m when the WLS was introduced into the volume of such a light guide, it rose to 4 m when a film WLS with varying thickness was used.[128]

When a film WLS is deposited on a light guide the latter can be immersed incompletely in a solution such that the part of it which extends beyond the sensitive scintillation volume is left "clean." Using a laminated light guide, this part was divided into strips, and from them by the method of heating and sintering a twisted light guide was prepared which in the end was compatible with the area of the photocathode.[127] Compared to an ordinary adiabatic light guide of the earlier calorimeter construction in Ref. 126, the new light guide with twisted "clean" part had higher light-collection efficiency and smaller contribution from Čerenkov radiation. In addition, this construction proved simpler to prepare and more reliable in operation. It should be added that in both types of these calorimeter modules the uniformity of light collection from the scintillators was improved by wrapping their surface adjacent to the light guide with black paper and then with aluminized Mylar. More specifically: the scintillation plates had dimensions $20\times20\times0.5$ cm, and black paper covered 5 cm of the end, which made it possible to somewhat lower the coefficient of light collection from the adjacent region. Conversely, the aluminumized Mylar gave some extra light arriving from distant points.

With decreasing thickness of the scintillation plate the number of reflections from the walls increases and, accordingly, the requirements on the quality of their surface get more stringent. For high uniformity of light collection it is also important that the plate thickness be constant. The high quality of the surface and fairly small tolerance in the thickness with the average value 2.5 mm of wafers of blue scintillator of the type B/PS (made by Bicron) are noted in Ref. 166. The uniformity of light collection by light guides with type-Y7 WLSs in two configurations has been compared for such plates of area 10×10 cm. In one of these the light was collected from the scintillator end by a laminated light guide, and in the other it was collected by a fiber imbedded in the scintillator, as shown in Fig. 5d. The two configurations gave similar results. However, the fiber variant, being less massive, is not as sensitive to Čerenkov radiation as the laminated variant. In addition, the information readout by means of a fiber makes it possible to section the calorimeter in the longitudinal direction. The fiber variant shown in Fig. 5c was used to construct a fine-grained calorimeter which is compact in the longitudinal direction.[36] But the coupling of the fibers to the scintillation plates is a rather complicated procedure.

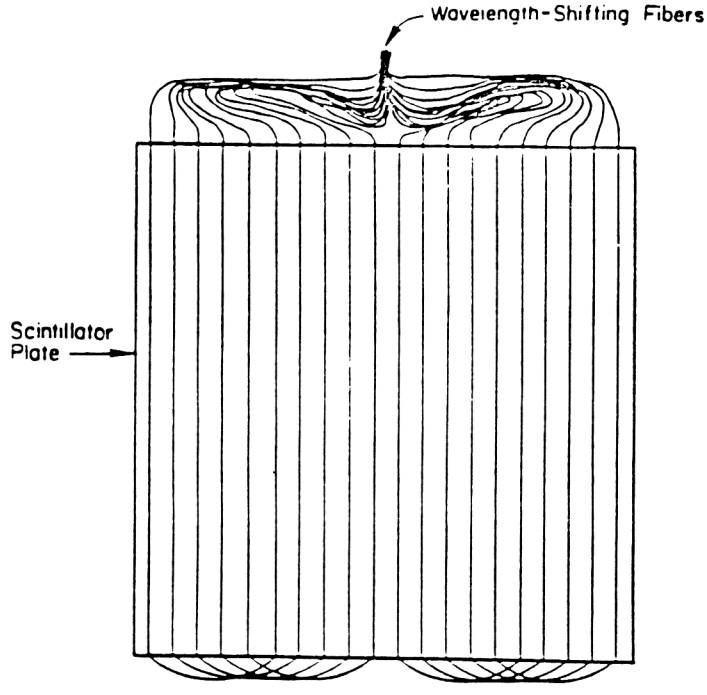

FIG. 12. Structure of the information readout from a scintillator of area 1 m^2 (Ref. 176).

The fiber configuration shown in Fig. 5e was used to construct a calorimeter from 4-mm-thick scintillator plates made of polyvinyltoluene scintillator of type BC-408 (Ref. 37). "Clean" fibers of length 4 m were optically connected to the fibers with WLSs at the scintillator outputs. Minimally ionizing particles gave at least 4 photoelectrons. The radiation strength of this laminated-fiber system was studied. After a 3-Mrad dose of gamma rays the light yield decreased roughly by half.

Attachment of the fiber in the shape of a U was used in Ref. 39 (see Fig. 5). An individual module of the calorimeter consisted of layers of lead and scintillator (SCSN18) of thicknesses 6.35 and 3 mm, respectively. The fiber contained a Y7-type of WLS with a concentration of 150 ppm. The resolution of the calorimeter in an electron beam was $\sigma/E = 0.2\sqrt{E[\text{GeV}]}$. After irradiation by a 2-GeV electron beam with a dose of 0.61 Mrad the average decrease of the pulse height was 19.3%.

The simplest U-shaped arrangement is realized in parallel grooves with the base of the letter U staggered, i.e., with the curves of the fibers lying outside the scintillator. For example, at Fermilab (Batavia, US) a calorimeter has been constructed using 3-mm-thick plates of large area, 1 m^2 (Ref. 176; see Fig. 12). Each scintillator (SCSN81) plate has 20 grooves. The first letter U occupies the first and sixth grooves, the second the second and seventh grooves, and so on. The uniformity over the 60×60 cm

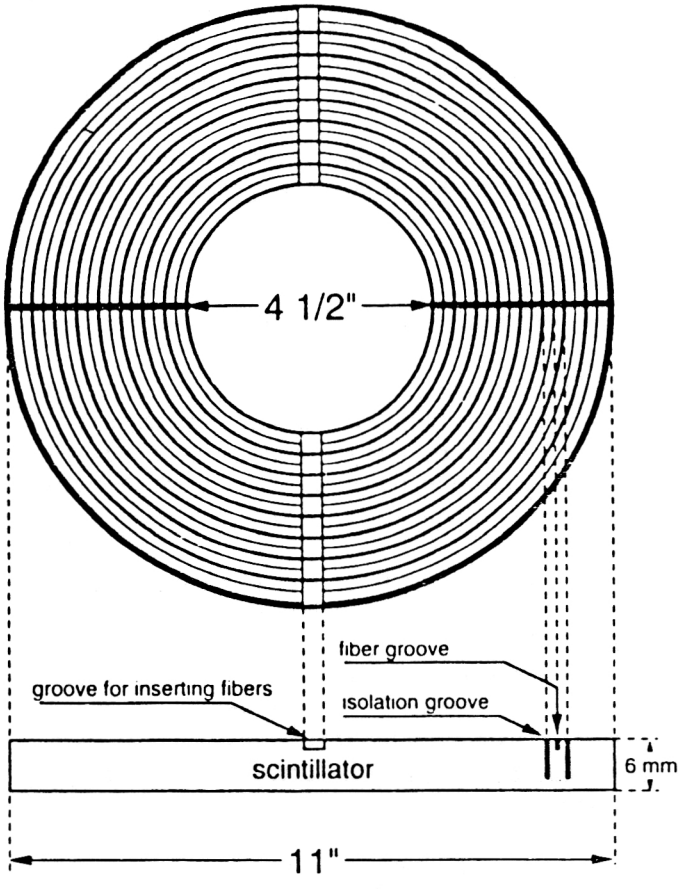

FIG. 13. Detector for locating the shower maximum (Ref. 158).

area was $\sigma=2$–5%. The calorimeter has a length of 2.2 m and consists of two parts. The first, which measures the electromagnetic shower energy $E_{\text{e.m.}}$, is made of 40 layers, and the second measures the hadronic shower energy E_{had}. The absorber (lead or iron) thickness is 3.2 mm. The total hadron energy is written as $E_{\text{total}}=E_{\text{e.m.}}+\alpha E_{\text{had}}$. The heights of the signals from each scintillation plate of the hadronic part were normalized in the information readout. In this way the resolution for a 240-GeV pion beam was improved from 7.8 to 6.9%; here $\alpha=4.9$. The resolution when iron absorbers were used turned out to be somewhat better than when lead ones were used, and was $\sigma/E(\%)=53.1/\sqrt{E}+4.1$.

An original scheme for light extraction from a scintillation plate by means of fibers containing WLSs was developed for a detector which determines the position of the maximum of an electromagnetic shower.[158] This device is shown in Fig. 13. The 6-mm-thick scintillator has the form of a disk with a hole inside and is divided into 8 parts by grooves of width 1.1 mm and depth 4.5 mm, which do not spoil the integrity of the scintillator. At the center of each part are grooves containing fibers with WLSs for information readout.

Scintillating-fiber calorimeters

As noted above, to obtain the ratio $e/h=1$ in a calorimeter made of layers of lead and scintillator the thicknesses of these layers must obey the ratio 4:1. However, here the thickness of the lead layers is rather large, and the contribution of sampling fluctuations becomes decisive in the energy resolution. To decrease this contribution it is necessary to decrease the thickness of the lead elements. The thickness of the scintillators must be decreased simultaneously. A natural solution to this technical problem is the use of scintillators in the form of fibers. This has been pursued, in particular, in the studies carried out for the LLA project at CERN (Refs. 154 and 159–163). Calorimeters with scintillating fibers have become known as "spaghetti calorimeters." The structure of such a calorimeter is shown in Fig. 14 (Ref. 161). Grooves for the fibers are made in the lead sheets. The assembly of sheets forms a matrix with a honeycomb structure of depth 2 m. Fibers of diameter 1 mm are located in it equidistantly with a spacing of 2.2 mm (Fig. 14a). The ratio of the volumes of lead and scintillator is 4:1. The fibers are grouped into sets of 1141 and form a tower with hexagonal cross section (86 mm between the sides). The 155 such towers form a 13-ton calorimeter with a diameter of about 1 m (Fig. 14b). The fibers are 2.2 m long and stick out of the back end of each tower. They are bunched together, machined and polished, and coupled through a light guide with a similar hexagonal shape (42 mm apex to apex and 79 mm long).

The fibers are laid along the shower at a small angle (3°) to its axis. The core of a fiber is made of SCSN38 scintillator, and the cladding is made of acrylic of thickness 29 μm. The cladding has smaller index of refraction than the core, which ensures light collection owing to total internal reflection at the boundary of the two media (see Sec.

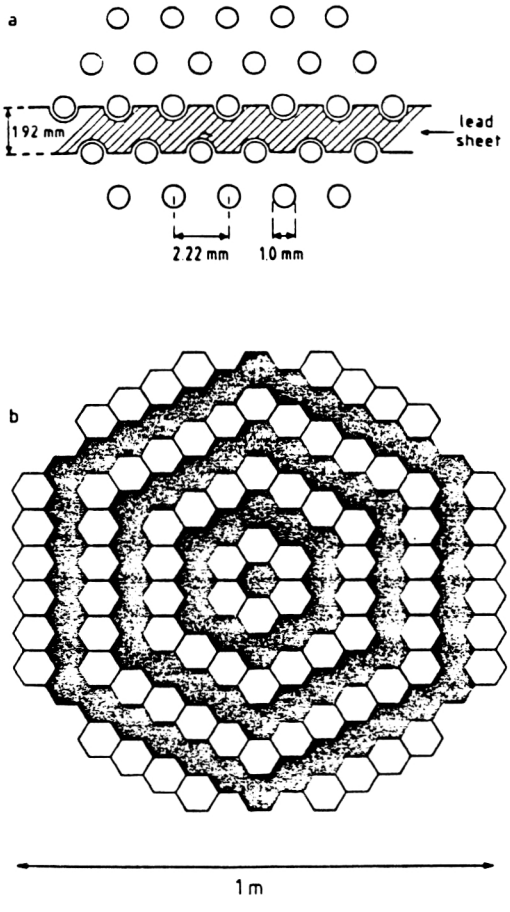

FIG. 14. Detail of (a) the face of the calorimeter and (b) the detector structure as a whole (Ref. 161).

2). The front ends of the fibers were polished, and an aluminum layer with high reflection coefficient equal to $85\pm4\%$ was deposited on them. To further increase the uniformity, a light filter absorbing short-wavelength light ($\lambda<450$ nm), which undergoes the maximum attenuation in transport along the fiber, was introduced. As a result, a light attenuation length of $\Lambda_0=7$ m was obtained.[163] Uniformity of the light collection along the fiber was particularly important because the calorimeter had no longitudinal segmentation. It was also important to sort the fibers into bundles for the individual modules with minimum fluctuations from fiber to fiber in their optical characteristics. The fibers were connected to XP2282 photomultipliers. The uniformity in the number of photoelectrons produced was better than 3% over the entire surface of a module. In the range 10–150 GeV the nonlinearity in measuring the magnitude of an electromagnetic shower was less than 1%. Here the energy resolution was $12.9\%/\sqrt{E}+a$, where $a=f(\theta_z)$ (Ref. 161). For a slope to the shower axis of $\theta_z=3°$, $a=1.2\%$. The constant term a arises from anomalous sampling fluctuations during the initial stage of shower development. It is strongly decreased when a preshower detector of thickness $1.7X_0$ (X_0 is the radiation length) is placed in front of the calorimeter. The resolution for pions was $30.6\%/\sqrt{E}+1\%$, where the second constant term arises mainly from light attenuation in the fibers. The coordinate resolution of the calorimeter for electrons and pions was $\sigma_e=17.1/\sqrt{E}$mm and $\sigma_\pi=(31.4/\sqrt{E}+2.4)$mm (Ref. 162).

The transverse segmentation of the calorimeter makes it possible to distinguish narrower electromagnetic showers from broader hadronic ones. In addition, electrons and π^- mesons can be separated on the basis of the difference in their time structure. The duration of a signal produced by electrons is 6–6.5 nsec (FWHM), and that of one produced by pions is 6–11 nsec (Ref. 159). Discrimination in the pulse shape is possible owing to the short luminescence time (1.5 nsec) of the scintillator used. If external light guides with WLSs were used the duration of the shifted scintillations would be increased significantly and discrimination in the pulse shape would become very difficult.

A coefficient of 10^{-4} is quoted in Ref. 162 for the separation of 80-GeV electrons and pions. The typical width of the "gates" passing signals to the amplitude analysis channel was 358 nsec. Narrowing of the gates to 40 nsec was accompanied by a significant deterioration of the calorimeter characteristics.[163] Nevertheless, it was noted that even for 15 nsec, the interval between beam bunches in the LHC and SSC colliders, this deterioration is not impossibly large.

One of the most difficult technical problems in working with such a complicated spectrometric detector as a calorimeter is controlling its stability and calibration. In a fiber detector this is achieved relatively simply: by replacing some of the scintillating fibers by wires of radioactive material. Here it is not difficult to arrange them such that the necessary number of gamma rays from a radioactive source hit all the fibers.

The use of scintillating fibers has made it possible to almost completely avoid the formation of "dead" zones in the calorimeter and to attain its maximum "hermiticity."

Among the drawbacks of fiber detectors is the relatively slow process of inserting fibers into lead. Accordingly, a technique for preparing a calorimeter by casting has been developed.[164] The fibers are stretched in a form into which the absorber is then poured. The absorber temperature must be low enough not to soften the fibers or damage their cladding. An alloy of lead with bismuth, tin, and cadmium (Pb-eutectic) is quite suitable. Its melting temperature is 70 °C, and its density is 9.5 g/cm^3. This alloy together with the fibers forms a homogeneous system which for a ratio of alloy and scintillator volumes of 4:1 has $X_0=0.9$ cm and a nuclear absorption length $\Lambda_1=22$ cm (for "pure" lead and scintillating wires, $X_0=0.75$ cm and $\Lambda_1=21$ cm). Small modules of dimensions $4\times4\times12$ cm were constructed. The calorimeter made of such modules had an energy resolution of $15–19\%/\sqrt{E}$ in an electron beam of energy 1.5–4 GeV. A similar technique has also been developed for the construction of liquid capillary calorimeters.

The type of calorimeter discussed above does not have longitudinal segmentation, although the difference in the longitudinal development of the showers they produce is used to seperate electrons and hadrons. A calorimeter with

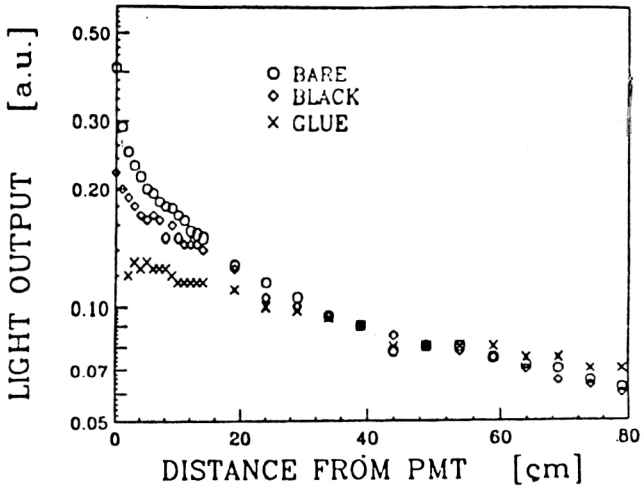

FIG. 15. Light yield of scintillating fibers with bare, blackened, and glued ends (see the text; Ref. 167).

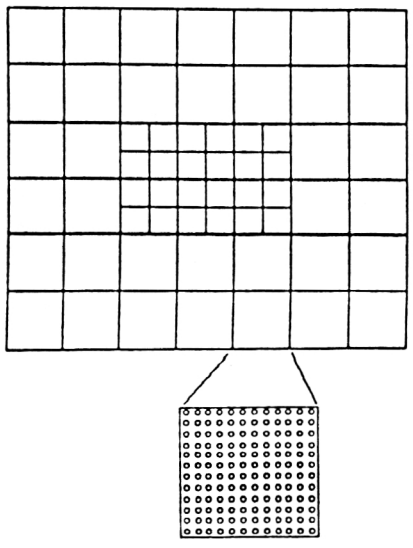

FIG. 16. Transverse cross section of a calorimeter with higher granularity of its central part. The transverse cross section of one module is also shown.[169]

transverse positioning of fibers in the lead volume has been built to achieve direct segmentation.[165] The light from the fibers is transported to photomultipliers by means of disks with WLSs positioned perpendicular to these fibers. This construction naturally leads to a decrease of the light collection compared to the case where the photomultipliers are directly connected to the fibers. In order to compensate for this loss, the disk thickness was increased from 2 to 3 mm. To preserve the optimal ratio (4:1) between the lead and scintillator thicknesses, the lead was also made a bit thicker. The energy resolution of the calorimeter in an electron beam of energy 1–2 GeV was $13.9\%/\sqrt{E}$. This value differs little from that obtained for a calorimeter with longitudinal placement of the fibers. However, the introduction of an additional light converter lowers the speed of response and the hermiticity of the setup, which is the price one must pay for direct segmentation of the calorimeter in the longitudinal direction.

Electromagnetic calorimeters with fiber light collection

If a lead-scintillator calorimeter is destined to measure the energy of only electromagnetic radiation, the question of compensation ceases to be relevant, and the resolution is improved by giving the scintillating fibers a large volume, for example, the same as for lead.[166] In this variant the resolution was improved to $\sigma = 6\%/\sqrt{E[\text{GeV}]}$ (Ref. 167). Here a fiber of diameter 1 mm was used, and the length of a module was $15X_0$, where $X_0 = 1.65$ cm. Measurements were made in a beam of photons of energy 20–80 MeV. The remarkable feature of the construction of this module is the method of improving the optical uniformity of the fibers.

As noted earlier, the light falling on the cladding also propagates to the photocathode owing to total internal reflection at the air boundary, although because of the optical imperfections of this surface the light is attenuated fairly rapidly. Nevertheless, near the edges closest to the photomultiplier there can be even more of this light than from the core, which is a source of nonuniformity. A significant suppression of the cladding light is obtained by blackening the ends of the fibers. However, it proved more effective simply to glue the surface at their ends (1.5 cm) to the lead, as illustrated in Fig. 15 (Ref. 167). A module which was similar but twice as long was made for a calorimeter designed to operate in the energy range 1–10 GeV.

The authors of Ref. 168 quote the resolution $\sigma/E(\%) = 13.1/\sqrt{E} + 1.7$ for a module of an electromagnetic calorimeter with a denser medium ($X_0 = 1.05$ cm). The fibers had a diameter of 1 mm and were arranged at an angle of 3° to the beam axis. The energy resolution of the module was studied for the electron beams of U-70 at ITEP and SPS at CERN in the energy range 5–70 GeV. The constant term in the expression for the resolution is mainly due to the attenuation in the fibers, which causes the number of photoelectrons to depend on the production point of the particles making up the shower. We see that at high energies ($E > 100$ GeV) the contribution of the constant term becomes dominant, which is characteristic also of other variants of electromagnetic calorimeters.

The fiber structure of the calorimeter simplifies its segmentation in the transverse direction for the purpose of determining the photon entry coordinates. For example, in Ref. 169 a calorimeter is described which consists of two types of modules with transverse cross sections of 25×25 mm and 12.5×12.5 mm (see Fig. 16), each respectively containing 144 and 36 fibers. One photomultiplier is connected to each such bundle. The next variant of the calorimeter[170] uses 16 modules of the first type (actually, with area 24×24 mm) in a 4×4 matrix. Four of them located at the center were additionally segmented along the X axis into three parts in order to improve the accuracy of determining the entry coordinates of the electromagnetic radiation. In other words, the central modules had an area

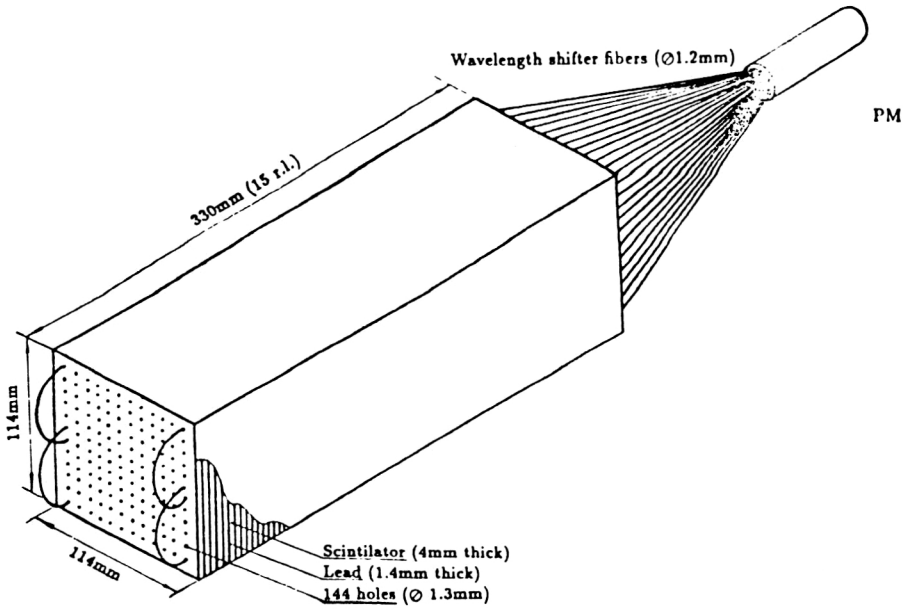

FIG. 17. A module of the calorimeter in Ref. 173.

of 8×24 mm. Scintillation wires (SCSF81) of diameter 1 mm were used. These were inserted into stainless steel tubes of inner diameter 1.1 mm and outer diameter 1.5 mm. The tubes were arranged with the appropriate spacing in a form into which AF-17 alloy of low melting temperature (96 °C) was poured. The composition of this alloy is 52.5% Bi+32.0% Pb+15.5% Sn. The radiation length was $X_0=0.91$ cm, and the length of the calorimeter was 35 cm.

The fibers were arranged so as to make a small angle relative to the direction of the detected electromagnetic radiation. The spatial resolution for electrons (2.4–8 GeV) incident on the central region was $\sigma_x = 2.8$ mm/$\sqrt{E[\text{GeV}]}$. Here the energy resolution was $\sigma/E = 18.5\%/\sqrt{E[\text{GeV}]}+1.9\%$.

A lead-scintillation cylindrical calorimeter with very short radiation length $X_0=0.75$ cm was built as an active screen for the VENUS detector located coaxially on the beam axis of the electron-positron collider TRISTAN (Ref. 171). Scintillating fibers of diameter 0.5 mm and $l=480$ mm were used. They were arranged in the lead along the beam. One end of the calorimeter had a well-machined smooth surface so that 16 plates containing WLSs could be placed right next to it. The shifted light was directed by these plates to four Hamamatsu R2940-4X photomultipliers having four anodes and operating in a parallel magnetic field. The calorimeter was used successfully both as a screen to shield from the background coming from the beam, and as a monitor of the beam luminosity.

The simplest and least expensive variant of electromagnetic calorimeter is composed of alternating layers of scintillator and lead. However, the nonuniformity of light collection in this variant strongly decreases the energy resolution. The uniformity of the light collection can be improved dramatically if the light is extracted by means of

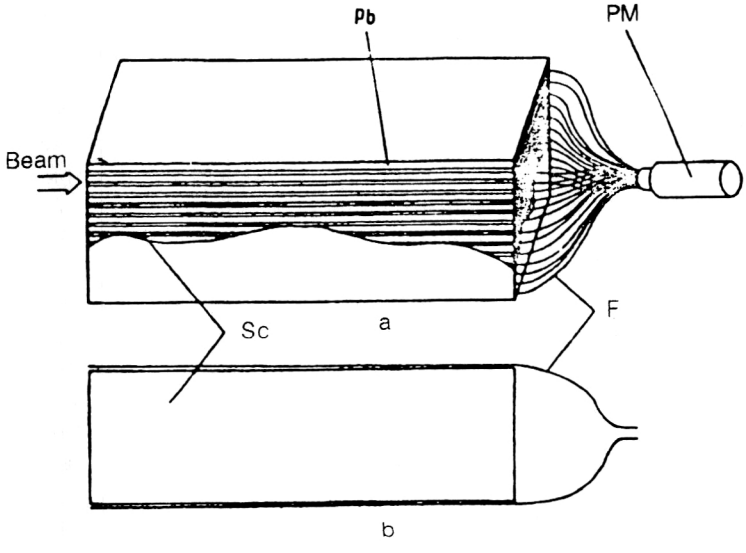

FIG. 18. Basic scheme of the calorimeter of Ref. 174 (a) and an individual scintillator (b). Sc is the scintillator, F is a fiber with wavelength shifter.

fibers containing WLSs (Refs. 172 and 173). Holes for the fibers to pass through are uniformly drilled throughout the entire surface area of the plates (Fig. 17). In Ref. 172 the calorimeter was constructed of 47 lead and 47 scintillator layers of area 70×70 cm. For a 2-mm-thick lead plates and 5-mm-thick scintillator plates the depth of the calorimeter was 17.3 r.l. The wires have diameter 1.5 mm and pass through 9 holes of diameter 2 mm. In Ref. 173 the number of holes was increased to 144, and their diameter was decreased to 1.3 mm for a wire diameter of 1.2 mm, which was achieved to within ±0.03 mm. The material forming the core of the fiber is polystyrene ($n_1=1.59$), and that of the cladding is PMMA ($n_2=1.40$). A scintillator with absorption spectrum at $\lambda=450$ nm and emission spectrum at $\lambda=530$ nm was dissolved in the polystyrene. The fibers are viewed from both sides, although they are connected to a single photodevice. This is accomplished by making a loop (3 cm in radius) on the face of the module. The losses in the loop are less than 5%, i.e., the loop acts as a mirror with coefficient of reflection greater than 95%. The effective attenuation length of the light was 1.2 m, and the surface nonuniformity was less than 2% For 1.4-mm-thick lead plates and 4-mm-thick scintillators the radiation length was 2.1 cm. In a beam of electrons of energy 0.5–5 GeV the energy resolution was $\sigma/E = 0.014 + 0.067/\sqrt{E}$, the time resolution was ~1 nsec, and the π/e rejection was at the level 10^{-2}–10^{-3}.

A calorimeter which is remarkably simple to make and assemble is shown in Fig. 18 (Ref. 174). Alternating plates of scintillator and lead are located along the beam at a small angle relative to it. A fiber with a shifter is connected from the outside to the scintillator faces. The bunched fibers are scanned by a single photomultiplier located in the back of the calorimeter. Here there is no need to use additional fiber light guides made of transparent material. A calorimeter module was made of 20 lead plates of dimensions $7\times20\times0.2$ cm alternating with scintillators of the same area and 0.1 cm thick. Experiments were performed in a beam of 26-GeV/c electrons. The quoted resolution was $\sigma/E = 21\%/\sqrt{E}$. This structure is particularly attractive for a hadronic calorimeter, and the possibility of constructing one of this type is being considered.

5. CONCLUSION

An important feature in recent years in physics at high, intermediate, and low energies is the construction of large-scale detectors of charged and neutral particles. Plastic scintillators have found extensive application here owing to important requirements on detectors such as speed of response and relatively low cost. In these characteristics plastic scintillators are significantly better than inorganic scintillating crystals, even though they are inferior to the latter as spectrometric detectors of electromagnetic radiation, particularly at low energies. Owing to its small value of Z, the efficiency of plastic for detecting gamma quanta is low. However, small Z is suitable for detecting low-energy electrons, since as Z increases their back scattering from the scintillator grows.

Charged-particle spectrometry is based primarily on detectors involving plastic scintillators. For particle paths of less than 20–30 cm, total-absorption detectors for measuring the particle energy are made from the "pure" scintillator. For particle identification, particularly in experiments with multiply charged ions, combinations of two scintillators with strongly differing luminescence times and connected to the same photomultiplier are often used. A fast scintillator is usually a plastic, and a slow one can be either a plastic or an inorganic crystal. The first variant is inferior to the second in resolution, but it can be used for high counting rates.

Most of the publications on detectors based on plastic scintillators are devoted to hadron calorimeters. Initially, such total-absorption detectors for showers generated by charged pions, protons, and other high-energy hadrons were constructed of alternating plates of scintillator and absorber: iron, copper, and, later, uranium and lead, which ensure better resolution. Here the light from the scintillators was transported to photomultipliers via light guides with a shifter in the form of a rod, a block, or a plate. A higher packing density is obtained by using fiber light guides or scintillating fibers instead of plates and placing them in a lead honeycomb structure along the particle beam. The last variant has the fastest speed of response, and the advantage of the first is the possibility of longitudinal segmentation of the calorimeter. Here its leading end can simultaneously perform the function of an electromagnetic calorimeter with sufficiently good energy resolution.

[1] J. B. Birks, *The Theory and Practice of Scintillation Counting* (Pergamon Press, London, 1964).
[2] Yu. K. Akimov, *Scintillation Counters in High Energy Physics* (Academic Press, New York, 1965) [Russian original, Moscow State University Press, Moscow, 1963)
[3] B. B. Govorkov and V. S. Chukin, Fiz. Elem. Chastits At. Yadra **3**, 763 (1972) [*sic*].
[4] F. D. Brooks, Nucl. Instrum. Methods **162**, 477 (1979).
[5] L. D. Landau, J. Phys. USSR **8**, 201 (1944).
[6] P. V. Vavilov, Zh. Eksp. Teor. Fiz. **32**, 920 (1957) [Sov. Phys. JETP **5**, 749 (1957)].
[7] P. Shulek, B. M. Golovin, L. A. Kulyukina *et al.*, Yad. Fiz. **4**, 564 (1966) [Sov. J. Nucl. Phys. **4**, 400 (1966)].
[8] J. F. Bak, A. Burenkov, J. B. B. Petersen *et al.*, Nucl. Phys. **B288**, 681 (1987).
[9] H. Bichsel, Rev. Mod. Phys. **60**, 663 (1988).
[10] H. Bichsel, Nucl. Instrum. Methods B **52**, 136 (1990).
[11] K. Yu. Akimov, Nucl. Instrum. Methods B **83**, 62 (1993).
[12] K. Nagata, T. Doke, J. Kikuchi *et al.*, Jpn. J. Appl. Phys. **14**, 697 (1975).
[13] J. H. Adams Jr., R. Silberberg, and G. D. Babhwar, Nucl. Instrum. Methods **124**, 551 (1975).
[14] Yu. K. Akimov, V. I. Komarov, O. V. Savchenko, and L. M. Soroko, Nucl. Instrum. Methods **7**, 37 (1960).
[15] D. Brini, L. Peli, and P. Veronesi, Nuovo Cim. Suppl. **2**, 1048 (1955).
[16] V. V. Ammosov, V. A. Gapienko, I. G. Golutvina *et al.*, Prib. Tekh. Eksp. No. 1, 94 (1990) [Instrum. Exp. Tech.].
[17] G. Bellettini, J. Budagov, F. Gervelli *et al.*, Preprint E13-93-296, JINR, Dubna (1993); submitted to Nucl. Instrum. Methods.
[18] R. L. Garwin, Rev. Sci. Instrum. **23**, 755 (1952).
[19] P. Gorenstein and D. Luckey, Rev. Sci. Instrum. **34**, 196 (1963).
[20] C. A. Gagliardi, R. E. Tribble, L. A. Van Ausdeln *et al.*, Nucl. Instrum. Methods A **273**, 117 (1988).
[21] Y. Lefevere, J. H. M. Bijleveld, M. Doets *et al.*, Nucl. Instrum. Methods A **290**, 34 (1990).
[22] G. Bendiscioli, V. Filippini, G. Fumagalli *et al.*, Nucl. Instrum. Methods **206**, 471 (1983).

[23] G. Bendiscioli, V. Filippini, C. Marciano *et al.*, Nucl. Instrum. Methods **227**, 478 (1984).
[24] A. Galiondo-Uribarri, T. E. Drake, G. C. Ball *et al.*, Nucl. Instrum. Methods A **301**, 457 (1991).
[25] F. Balestra, M. P. Bussa, L. Bussa *et al.*, Nucl. Instrum. Methods A **234**, 30 (1985).
[26] W. A. Schurclif, J. Opt. Soc. Am. **41**, 209 (1951).
[27] R. C. Garwin, Rev. Sci. Instrum. **31**, 1010 (1960).
[28] G. Keil, Nucl. Instrum. Methods **83**, 145 (1970); **89**, 111 (1970).
[29] B. Barish, A. Bodek, Y. K. Chu *et al.*, IEEE Trans. Nucl. Sci. **NS-29**, 532 (1978).
[30] V. Eckardt, R. Kalbach, A. Manz *et al.*, Nucl. Instrum. Methods **155**, 389 (1978).
[31] W. Selove, W. Kononenko, and B. Wilsker, Nucl. Instrum. Methods **161**, 233 (1979).
[32] J. Fent, H. Fessler, P. Freund *et al.*, Nucl. Instrum. Methods **211**, 315 (1983).
[33] H. Fessler, P. Freund, J. Gebauer *et al.*, Nucl. Instrum. Methods **228**, 303 (1985).
[34] V. I. Kryshkin and A. I. Ronzhin, Nucl. Instrum. Methods A **247**, 583 (1986).
[35] M. G. Albrow, G. Arnison, J. Bunn *et al.*, Nucl. Instrum. Methods A **256**, 23 (1987).
[36] J. Simon-Gillo, A. Farooq, M. W. Rawool *et al.*, Nucl. Instrum. Methods A **309**, 427 (1991).
[37] P. De Barbaro, A. Bodeck, R. S. Budd *et al.*, Nucl. Instrum. Methods A **315**, 317 (1992).
[38] P. Klasen, K. Kleinknecht, and D. Pollmann, Nucl. Instrum. Methods **185**, 67 (1981).
[39] G. R. Young, T. S. Awes, C. Baktash *et al.*, Nucl. Instrum. Methods A **279**, 503 (1989).
[40] A. N. Vasil'ev, N. K. Vishnevskiĭ, P. N. Kazakov *et al.*, Preprint No. 82-62 OÉF, IHEP, Serpukhov (1982) [in Russian].
[41] T. Kamon, K. Kondo, A. Yamashita *et al.*, Nucl. Instrum. Methods **213**, 261 (1983).
[42] S. Bertolucci, M. Cordelli, B. Esposito *et al.*, Nucl. Instrum. Methods A **267**, 301 (1988).
[43] C. L. Renschler and L. A. Harrah, Nucl. Instrum. Methods A **235**, 41 (1985).
[44] E. A. Andreeshchev, S. F. Kilin, Yu. P. Kushakevich *et al.*, Prib. Tekh. Eksp. No. 6, 35 (1982) [Instrum. Exp. Tech.].
[45] I. A. Berezin, V. M. Gorbachev, V. V. Nazarov *et al.*, Prib. Tekh. Eksp. No. 1, 53 (1981) [Instrum. Exp. Tech.].
[46] V. A. Zyablin, S. F. Kilin, A. F. Kulakova *et al.*, Prib. Tekh. Eksp. No. 2, 73 (1986) [Instrum. Exp. Tech.].
[47] T. Hasegawa, M. Hazumi, S. Kasai *et al.*, Nucl. Instrum. Methods A **311**, 498 (1992).
[48] E. Bodenstedt, L. Ley, H. O. Schlenz, and E. Wahman, Nucl. Phys. **A137**, 33 (1966).
[49] E. Jeenicke, P. Liaud, B. Vignon, and R. Wilson, Nucl. Instrum. Methods **126**, 459 (1975).
[50] E. Johnson, R. E. Merrifield, P. Avakian, and R. Flippen, Phys. Rev. Lett. **19**, 285 (1979).
[51] S. Bertolucci, M. Cordelli, M. Curatolo *et al.*, Nucl. Instrum. Methods A **254**, 561 (1987).
[52] D. Blömker, U. Holm, B. Klanmer, and B. Krobs, IEEE Trans. Nucl. Sci. **NS-37**, 220 (1990).
[53] J. P. Cumalat, H. W. K. Cheung, J. Hassed *et al.*, Nucl. Instrum. Methods A **293**, 606 (1990).
[54] J. Mainush, F. Corriveau, R. Klanner, and G. Levman, Nucl. Instrum. Methods A **312**, 451 (1992).
[55] H. Schonbacher and W. Witzeling, Nucl. Instrum. Methods **169**, 517 (1979).
[56] Y. Sirois and R. Wigmans, Nucl. Instrum. Methods A **240**, 262 (1985).
[57] R. Klanner, Nucl. Instrum. Methods A **265**, 200 (1988).
[58] C. Zorn, M. Bowen, S. Majewski *et al.*, Nucl. Instrum. Methods A **273**, 108 (1988).
[59] U. Holm and K. Wick, IEEE Trans. Nucl. Sci. **NS-36**, 579 (1989).
[60] K. Wick, G. Riedel, D. Paul, and V. Stieber, Nucl. Instrum. Methods A **277**, 251 (1989).
[61] S. Majewski, M. Bowen, J. Szaban, and C. Zorn, Nucl. Instrum. Methods A **281**, 497 (1989).
[62] S. Majewski, M. Bowen, C. Zorn *et al.*, *ibid.*, p. 500.
[63] C. Zorn, M. Bowen, S. Majewski *et al.*, IEEE Trans. Nucl. Sci. **NS-37**, 557 (1990).
[64] M. Bowen, S. Majewski, D. Pettey *et al.*, *ibid.*, p. 562.
[65] V. M. Feygelman, J. K. Walker, and J. P. Harmon, Nucl. Instrum. Methods A **290**, 131 (1990).
[66] V. M. Feygelman, J. K. Walker, J. P. Harmon *et al.*, Nucl. Instrum. Methods A **295**, 94 (1990).
[67] K. F. Jonson and H. L. Whitaker, Nucl. Instrum. Methods A **301**, 372 (1991).
[68] A. D. Bross, A. Pla-Dalmau, B. Baumbaugh *et al.*, Nucl. Instrum. Methods A **307**, 35 (1991).
[69] J. Piekarz, in *Proc. of the Symp. on Detector Research and Development for the SSC*, 1990, Fort Worth, Texas, p. 281.
[70] J. K. Walker, J. P. Harmon, C. W. Park, and S. Li, *ibid.*, p. 294.
[71] R. L. Cough and J. S. Wallace, *ibid.*, p. 661.
[72] M. Bertoldi, Goforth, V. Hagopian *et al.*, *ibid.*, p. 674.
[73] K. F. Jonson, D. W. Hertzog, S. A. Hughes *et al.*, *ibid.*, p. 672.
[74] A. D. Bross, A. Pla-Dalmau, and C. W. Spangler, Nucl. Instrum. Methods A **325**, 168 (1993).
[75] A. D. Bross and A. Pla-Dalmau, Nucl. Instrum. Methods A **327**, 337 (1993).
[76] G. I. Britvich, A. I. Peresypkin, V. I. Rykalin *et al.*, Nucl. Instrum. Methods A **326**, 483 (1993).
[77] G. Marin *et al.*, CERN Report 85-08, CERN, Geneva (1985).
[78] Yu. D. Bayukov, A. E. Bukleĭ, V. B. Gavrilov *et al.*, Preprint ITEP-15, ITEP, Moscow (1980) [in Russian].
[79] G. F. Hartner, D. F. Blodgett, S. B. Bracker *et al.*, Nucl. Instrum. Methods **216**, 113 (1983).
[80] J. D. MacGregor, S. N. Dancer, J. R. M. Annand *et al.*, Nucl. Instrum. Methods A **262**, 347 (1987).
[81] F. M. Rozon, N. Grion, and R. Rui, Nucl. Instrum. Methods A **267**, 101 (1988).
[82] Yu. P. Antipov, N. P. Budanov, Yu. P. Gorin *et al.*, Prib. Tekh. Eksp. No. 5, 36 (1988) [Instrum. Exp. Tech.].
[83] Yu. K. Akimov, I. I. Gaĭsak, D. Dorchioman *et al.*, Prib. Tekh. Eksp. No. 4, 24 (1981) [Instrum. Exp. Tech.].
[84] A. Baden, H. H. Gudbrod, H. Löhner *et al.*, Nucl. Instrum. Methods A **203**, 189 (1982).
[85] D. H. Wilkinson, Rev. Sci. Instrum. **23**, 414 (1952).
[86] D. Bodansky and S. F. Eccles, Rev. Sci. Instrum. **28**, 464 (1957).
[87] C. Pastor, F. Benrachi, B. Chambon *et al.*, Nucl. Instrum. Methods **212**, 209 (1983).
[88] C. Pastor, F. Benrachi, B. Chambon *et al.*, Nucl. Instrum. Methods **227**, 87 (1984).
[89] J. Alarja, A. Danchy, A. Giorni *et al.*, Nucl. Instrum. Methods A **242**, 352 (1986).
[90] H. K. W. Leegte, E. E. Koldenhof, A. L. Boonstra, and H. M. Wilschut, Nucl. Instrum. Methods A **313**, 26 (1992).
[91] F. Liden, J. Nyberg, A. Jonson, and A. Kerek, Nucl. Instrum. Methods **253**, 305 (1987).
[92] E. Migneco, C. Agodi, R. Alba *et al.*, Nucl. Instrum. Methods A **314**, 31 (1992).
[93] D. G. Sarantites, L. G. Sobotka, T. M. Semkow *et al.*, Nucl. Instrum. Methods A **264**, 319 (1988).
[94] D. W. Stracener, D. G. Sarantites, L. G. Sobotka *et al.*, Nucl. Instrum. Methods A **294**, 485 (1990).
[95] E. Norbeck, T. P. Dubbs, and L. G. Sobotka, Nucl. Instrum. Methods A **262**, 546 (1987).
[96] C. A. Pruneau, G. C. Ball, P. Dmytrenko *et al.*, Nucl. Instrum. Methods A **297**, 404 (1990).
[97] R. T. De Souza, N. Carlin, Y. D. Kim *et al.*, Nucl. Instrum. Methods A **295**, 109 (1990).
[98] J. L. Langenbrunner, C. L. Morris, and R. M. Whitton, Nucl. Instrum. Methods A **316**, 450 (1992).
[99] G. Lanzano, A. Pagano, E. De Filippo *et al.*, Nucl. Instrum. Methods A **323**, 694 (1992).
[100] Y. Futami, T. Mizota, Y. H. Pu *et al.*, Nucl. Instrum. Methods A **326**, 513 (1993).
[101] N. N. Ajitanand, M. Beuhler, C. Gelderloos, and J. M. Alexander, Nucl. Instrum. Methods A **316**, 446 (1992).
[102] P. J. Ebert, A. F. Lanzon, and E. N. Lent, Phys. Rev. **183**, 422 (1969).
[103] T. Tabata, Phys. Rev. **162**, 336 (1967).
[104] J. C. Trump and K. Wright, J. Appl. Phys. **33**, 687 (1962).
[105] C. D. Zerby and F. L. Keller, Nucl. Sci. Eng. **27**, 190 (1967).

[106] M. J. Saltmarsh, B. M. Predom, R. D. Edge, and C. W. Darden, Nucl. Instrum. Methods **105**, 311 (1972).
[107] D. Axen, G. Duesdieker, L. Felawka *et al.*, Nucl. Instrum. Methods **118**, 435 (1974).
[108] Yu. K. Akimov, S. I. Merzljakov, K. O. Oganesjan *et al.*, Preprint E13-80-10, JINR, Dubna (1980).
[109] V. Bernard, J. Girard, J. Julien *et al.*, Nucl. Phys. **A423**, 511 (1984).
[110] Particle Data Group, Phys. Lett. **B239**, 1116 (1990).
[111] Yu. K. Akimov, A. S. Kuznetsov, and G. A. Leksin, Prib. Tekh. Eksp. No. 2, 70 (1956) [Instrum. Exp. Tech.].
[112] N. L. Grigorov, V. S. Murzin, and I. D. Rapoport, Zh. Eksp. Teor. Fiz. **34**, 508 (1958) [Sov. Phys. JETP **7**, 350 (1958)].
[113] T. Massam, Th. Muller, M. Schneegans, and A. Zichichi, Nuovo Cimento **39**, 464 (1965).
[114] A. Zichichi, Ann. Phys. (N.Y.) **66**, 405 (1971).
[115] M. Basile, J. Berbiers, D. Bollini *et al.*, Nucl. Instrum. Methods **101**, 433 (1972).
[116] W. Hofmann, J. Spengler, D. Wegener *et al.*, Nucl. Instrum. Methods **163**, 77 (1979).
[117] M. A. Scheegans, J. J. Aubert, G. Coignet *et al.*, Nucl. Instrum. Methods **193**, 445 (1982).
[118] Yu. K. Akimov, Fiz. Elem. Chastits At. Yadra **25**, 229 (1994) [Sov. J. Part. Nucl. **25**, 92 (1994)].
[119] J. Engler, W. Flauger, B. Gibbard *et al.*, Nucl. Instrum. Methods **106**, 189 (1973).
[120] M. Holder, J. Knobloch, and J. May, Nucl. Instrum. Methods **151**, 69 (1978).
[121] P. Bother, S. Dagan, C. W. Fabjan *et al.*, Nucl. Instrum. Methods **179**, 45 (1981).
[122] H. Abramowicz, J. G. H. de Groot, J. Knobloch *et al.*, Nucl. Instrum. Methods **180**, 429 (1981).
[123] G. Bellettini, R. Bertani, C. Bradaschia *et al.*, Nucl. Instrum. Methods **204**, 73 (1982).
[124] M. De Vincenzi, S. Di Liberto, A. Frankel *et al.*, Nucl. Instrum. Methods A **248**, 326 (1986).
[125] T. Binon, C. Bricman, V. M. Buyanov *et al.*, Nucl. Instrum. Methods A **256**, 444 (1987).
[126] V. S. Datsko, S. V. Donskov, A. V. Inyakin *et al.*, Preprint 87-85, IHEP, Serpukhov (1987) [in Russian].
[127] S. I. Bityukov, V. K. Semenov, and A. P. Yablokov, Prib. Tekh. Eksp. No. 4, 58 (1989) [Instrum. Exp. Tech.].
[128] T. C. Awes, C. Baktash, R. P. Cumby *et al.*, Nucl. Instrum. Methods A **279**, 479 (1989).
[129] Yu. M. Antipov, P. Cantoni, V. S. Datsko *et al.*, Nucl. Instrum. Methods A **295**, 81 (1990).
[130] I. Kudla, R. J. Nowak, R. Walczak *et al.*, Nucl. Instrum. Methods A **300**, 408 (1991).
[131] M. Derrick, D. Gasek, B. Musgrave *et al.*, Nucl. Instrum. Methods A **309**, 77 (1991).
[132] O. P. Gavrishchuk, R. V. Eremeev, M. G. Kadykov *et al.*, Prib. Tekh. Eksp. No. 3, 37 (1993) [Instrum. Exp. Tech.].
[133] C. W. Fabjan, W. Struczinski, W. J. Willis *et al.*, Nucl. Instrum. Methods **141**, 61 (1977).
[134] P. Bother, V. Burkert, A. Di Ciaccio *et al.*, IEEE Trans. Nucl. Sci. **NS-29**, 373 (1982).
[135] C. W. Fabian and T. Lundlam, Ann. Rev. Nucl. Sci. **32**, 335 (1982).
[136] T. Akesson, R. Batley, O. Benary *et al.*, Nucl. Instrum. Methods A **241**, 17 (1987).
[137] T. Akesson, A. L. S. Angelis, F. Corriveau *et al.*, Nucl. Instrum. Methods A **262**, 243 (1987).
[138] G. D'Agostini *et al.*, Nucl. Instrum. Methods A **274**, 134 (1989).
[139] G. R. Young, T. C. Awes, C. Baktash *et al.*, Nucl. Instrum. Methods A **279**, 503 (1989).
[140] U. Behrens, J. Crittenden, K. Dierks *et al.*, Nucl. Instrum. Methods A **289**, 115 (1990).
[141] A. Andresen *et al.*, Nucl. Instrum. Methods A **290**, 95 (1990).
[142] B. G. Bylsma, L. S. Durkin, T. A. Romanowski, and R. Seidlen, Nucl. Instrum. Methods A **305**, 354 (1991).
[143] The ZEUS Calorimeter Group, Nucl. Instrum. Methods A **309**, 101 (1991); **315**, 311 (1992); **320**, 161 (1992).
[144] R. Wigmans, Nucl. Instrum. Methods A **259**, 389 (1987).
[145] E. Bernardi, G. Drews, M. A. Garcia *et al.*, Nucl. Instrum. Methods A **262**, 229 (1987).
[146] M. E. Duffy, G. K. Fanourakis, R. J. Loveless *et al.*, Nucl. Instrum. Methods **228**, 37 (1984).
[147] H. Tiecke, Nucl. Instrum. Methods A **277**, 42 (1989).
[148] G. Drews, M. A. Garcia, R. Klanner *et al.*, Nucl. Instrum. Methods A **290**, 335 (1990).
[149] J. P. Sullivan, M. W. Rawool-Sullivan, and J. G. Boissevain, Nucl. Instrum. Methods A **324**, 441 (1993).
[150] A. Zichichi, Riv. Nuovo Cimento **13**, No. 5 (1990).
[151] R. DeSalvo, F. G. Hartjes, A. M. Henriques *et al.*, Nucl. Instrum. Methods A **279**, 467 (1989).
[152] P. K. Job, L. Price, J. Proudfoot *et al.*, Nucl. Instrum. Methods A **309**, 60 (1991).
[153] P. K. Job, L. Price, J. Proudfoot *et al.*, Nucl. Instrum. Methods A **316**, 174 (1992).
[154] M. Hirschberg, R. Beckmann, U. Brandenburg *et al.*, IEEE Trans. Nucl. Sci. **NS-39**, 511 (1992).
[155] A. N. Vasil'ev, N. K. Vishnevskiĭ, P. N. Kazakov *et al.*, Preprint 82-62, OÉF, IHEP, Serpukhov (1982).
[156] C. Aurouet, H. Blumenfeld, G. Bosc *et al.*, Nucl. Instrum. Methods, Vol. 169, p. 57 (1980).
[157] O. Bother, S. Dagan, C. W. Fabjan *et al.*, Nucl. Instrum. Methods **179**, 45 (1981).
[158] G. Appollinari, N. D. Giokaris, K. Goulianos *et al.*, Nucl. Instrum. Methods A **324**, 475 (1993).
[159] A. Zichichi, Riv. Nuovo Cim. **13**, Nos. 10–11 (1990).
[160] D. Acosta, S. Buontempo, L. Caloŏba *et al.*, Nucl. Instrum. Methods A **294**, 193 (1990); **302**, 36 (1991); **305**, 55 (1991); **308**, 481 (1991).
[161] D. Acosta, P. Avellino, S. Buontempo *et al.*, Nucl. Instrum. Methods A **309**, 143 (1991); **314**, 431 (1992).
[162] R. Wigmans, in *Proc. of the Symp. on Detector Research and Development for the SSC*, 1990, Fort Worth, Texas, p. 281.
[163] H. P. Paar, *ibid.*, p. 391.
[164] W. Worstell, J. Miller, L. Roberts *et al.*, *ibid.*, p. 428.
[165] J. Proudfoot, P. K. Job, H.-J. Trost *et al.*, *ibid.*, p. 410.
[166] R. McNeil, A. Fazely, R. Gunasingha *et al.*, *ibid.*, p. 435.
[167] S. Bianco, R. Casaccia, L. Daniello *et al.*, Nucl. Instrum. Methods A **315**, 322 (1992).
[168] J. Budagov, I. Chirikov-Zorin, V. Glagolev *et al.*, Preprint E13-93-308, JINR, Dubna (1993) [in Russian] (submitted to Nucl. Instrum. Methods).
[169] M. Bertino, C. Bini, D. De Pedis *et al.*, Nucl. Instrum. Methods A **315**, 327 (1992).
[170] A. Asmone, M. Bertino, C. Bini *et al.*, Nucl. Instrum. Methods A **326**, 477 (1993).
[171] F. Takasaki, T. Utsumi, T. Fukui *et al.*, Nucl. Instrum. Methods A **322**, 211 (1992).
[172] S. V. Afanas'ev, V. A. Gladyshev, and A. E. Zatserklyanyĭ, Prib. Tekh. Eksp. No. 5, 63 (1992) [Instrum. Exp. Tech.].
[173] G. S. Atoyan, V. A. Gladyshev, S. N. Gninenko *et al.*, Nucl. Instrum. Methods A **320**, 144 (1992).
[174] V. I. Kryshkin, V. G. Lapshin, A. I. Mysnik *et al.*, Prib. Tekh. Eksp. No. 3, 43 (1993) [Instrum. Exp. Tech.].
[175] J. B. Costales, H. C. Britt, M. N. Namboodiri *et al.*, Nucl. Instrum. Methods A **330**, 183 (1993).
[176] A. Beretvas, A. Byon-Wagner, and G. W. Foster, Nucl. Instrum. Methods A **329**, 50 (1993).

Translated by Patricia A. Millard